ES cells recovered completely to the level of wild-type EB3 ES cells (Fig. 3C-E). Essentially similar inhibitory effects of Smad7 expression on mES cell propagation were observed using another clone fSmad7-7 (data not shown). Although stable expression of Smad7 interferes with mES growth, cell-cycle distribution of fSmad7-10$^+$, fSmad7-10$^-$ and EB3 ES cells was not significantly altered (data not shown). These results clearly indicate that the inhibitory effect of Smad7 on proliferation of mES cells is completely reversible.

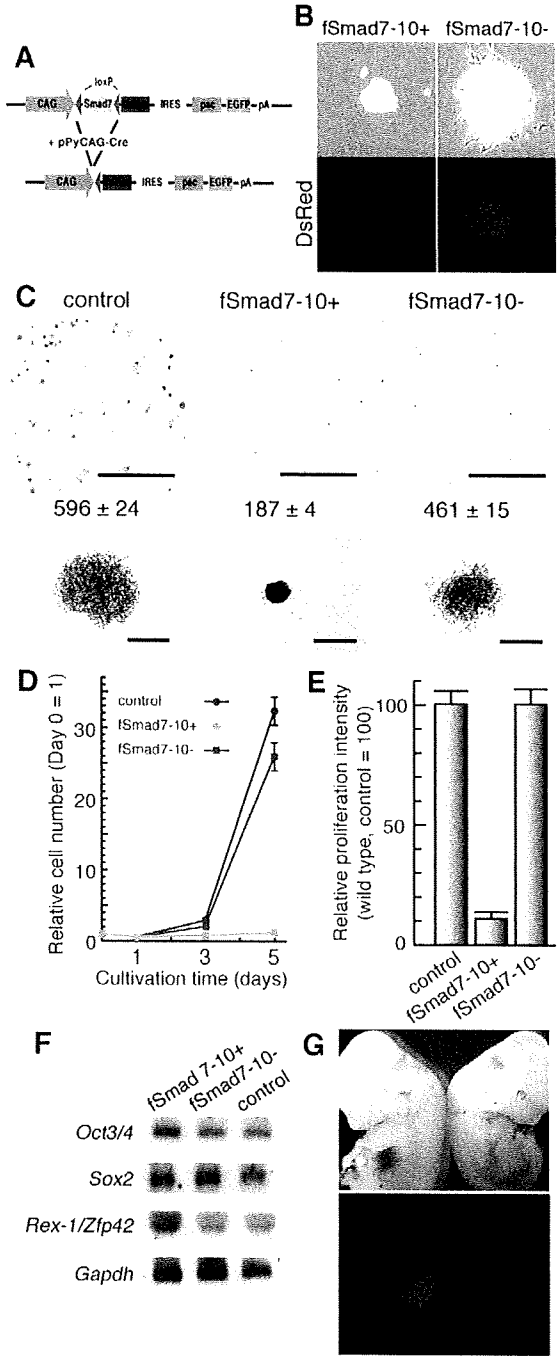

The growth-inhibitory effect of Smad7 does not affect pluripotency of mES cells

To determine whether the undifferentiated state of mES cells was retained during reversible expression of the Smad7 transgene, we prepared RNA from these ES cells and investigated the expression of three stem-cell-specific genes, *Oct3/4* (Niwa et al., 2000; Niwa et al., 2002), *Sox2* (Yuan et al., 1995) and *Zfp42/Rex1* (Rogers et al., 1991) by northern blot analysis. All stem cell marker genes were strongly expressed in both Smad7-10$^+$ and Smad7-10$^-$ ES cells (Fig. 3F) although there were differences in their expression levels (supplementary material Fig. S2). To confirm the maintenance of pluripotency in these cells, DsRed-expressing fSmad7-10$^-$ ES cells were injected into blastocysts obtained from C57BL/6 strain mice. Embryos with DsRed fluorescence were successfully obtained, suggesting that the pluripotency of Smad7-10$^-$ ES cells contributing to embryogenesis (Fig. 3G, left, compared with control littermates). These results indicate that temporary forced expression of *Smad7* does not affect the pluripotency of ES cells.

Negative effect of forced *Smad7* expression depends in part on TGFβ-related activity in FCS

We showed that activin-Nodal-TGFβ signaling is autonomously activated in ES cells in FCS-containing medium (Fig. 1A). We next examined whether this activation results from the agents included in FCS-containing medium. We recently demonstrated that ES cells, when cultured without FCS in serum-free medium supplemented with KSR, LIF, and ACTH, can propagate even from single cells (clonal density <25 cells/cm^2) with proper pluripotency (Ogawa et al., 2004). Since serum-free medium contains no TGFβ-related molecules, we used it to investigate whether the

Fig. 3. The inhibitory effect of Smad7 is reversible. (A) Strategy for generation of fSmad7-10$^+$ and fSmad7-10$^-$ ES cells. fSmad7-10$^+$ was generated by stable integration of floxed-*Smad7* cDNA transgene under the CAG promoter into EB3 ES cells. After elctroporation of pCAGGS-Cre into fSmad7-10$^+$, fSmad7-10$^-$ was free of *Smad7* cDNA and expressed DsRed. (B) Colony morphologies of fSmad7-10$^+$ (left) and Smad7-10$^-$ (right) cells. EB3 (control), fSmad7-10$^+$ and fSmad7-10$^-$ ES cells were seeded at 2000 cells/well in six-well plates, and cultured for 1 week in the medium supplemented with puromycin. The lower panel shows expression of DsRed. (C) Colony morphologies of fSmad7-10$^+$, fSmad7-10$^-$, and control ES cells. fSmad7-10$^+$ (middle), fSmad7-10$^-$ (right) and EB3 (as control, left) ES cells were cultured in FCS-containing medium for 5 days. Numbers indicate numbers of colonies appearing (n=3). The lower panel shows AP staining. Bars, 5 mm (upper panels); 200 μm (lower panels). (D) Relative numbers of each transfectant present on Days 1, 3, and 5 of culture compared with Day 0. Each bar represents the mean ± s.e.m. (n=4). (E) Relative proliferation intensity is shown as total cell number on Day 5/number of colonies appearing, compared with that of EB3 ES cells (100%). Each bar represents the mean ± s.e.m. (n=3). (F) Expression of stem cell marker genes *Oct3-4*, *Sox2*, and *Rex-1* in fSmad7-10$^+$, fSmad7-10$^-$ and EB3 (as control) ES cells examined by northern blot analysis. ES cells were cultured in FCS-containing medium for 5 days. *Gapdh* was detected as a loading control. (G) Chimeric mice derived from fSmad7-10$^-$ cells that had been cultured for at least 1 month. Chimeric mice (upper panel) expressed DsRed, whereas control mice (lower panel) exhibited no DsRed fluorescence.

negative effect of forced *Smad7* expression depends on TGFβ-related activity in FCS. In serum-free medium, although proliferation of fSmad7-10$^+$ cells was slower than that of fSmad7-10$^-$ cells and wild-type EB3 ES cells, the inhibitory effect of forced *Smad7* expression was reduced compared with that in FCS-containing medium (compare Fig. 3E with Fig. 4C). These results indicate that the growth-inhibitory effect of forced *Smad7* expression is partly due to the blockade of signaling from soluble TGFβ-related molecules in FCS that promote ES cell propagation.

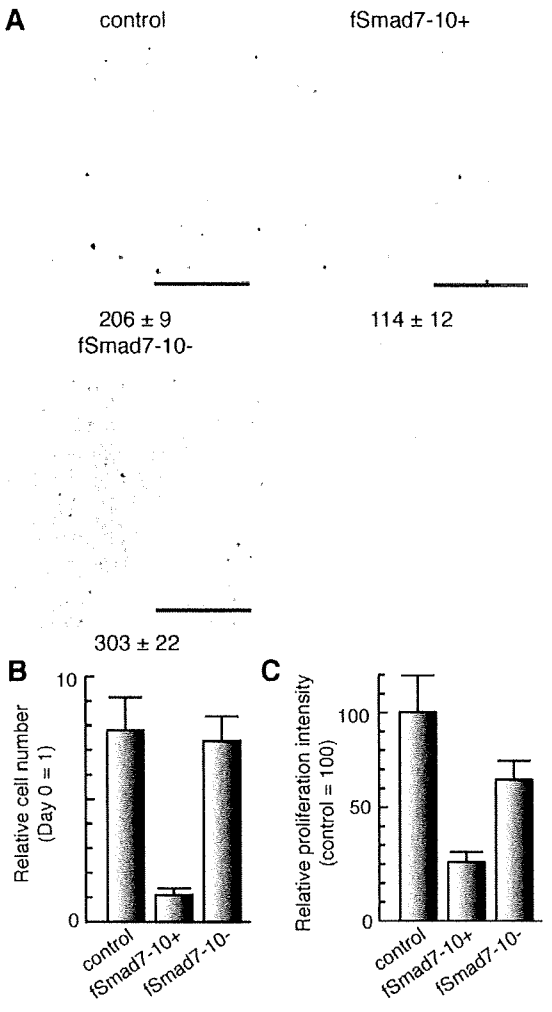

Fig. 4. Inhibitory effect of Smad7 in serum-free conditions. (A) Colony morphologies of fSmad7-10$^+$ and fSmad7-10$^-$ ES cells in serum-free medium. fSmad7-10$^+$ (middle), fSmad7-10$^-$ (right), and EB3 (as control, left) ES cells were seeded at 2000 cells/well in six-well plates, and cultured in FCS-containing medium for 1 week. Numbers indicate numbers of colonies appearing (n=3). Bars, 5 mm. (B) Relative numbers of each transfectant present on Day 7 of culture compared with Day 0. Each bar represents the mean ± s.e.m. (n=4). (C) Relative proliferation intensity is shown as total cell number/number of colonies appearing, compared with that of EB3 ES cells (100%). Each bar represents the mean ± s.e.m. (n=3).

Exogenous Nodal and activin promote ES cell propagation in serum-free conditions

We next attempted to enhance ES cell proliferation by stimulating activin-Nodal-TGFβ signaling using exogenous ligands. To determine whether ES cells are capable of transducing TGFβ superfamily signals, we examined the expression of various TGFβ superfamily signaling components in mES cells by RT-PCR analysis (supplementary material Fig. S3). We detected transcripts of all of the TGFβ superfamily ligands except activin-βA and TGF-β3, suggesting that ES cells produce TGFβ superfamily ligands by themselves, at least at the transcriptional level. We also detected transcripts of type I and II receptors for activin-Nodal and BMPs but not ALK-7, which is known to be a specific receptor for Nodal, in MGZ5 and EB5 ES cells. However, we detected transcripts of Cripto-1 in these ES cells, suggesting that Nodal signaling can be transduced in ES cells via ALK-4 (Yan et al., 2002). By contrast, transcripts of type II TGFβ receptors were not detected, as has been previously reported (Goumans et al., 1998), suggesting that ES cells are not capable of responding to TGFβ ligands. However, transcripts of all types of Smads were detected, suggesting that ES cells are capable of responding to activin, Nodal and BMP.

We next examined whether exogenous TGFβ superfamily ligands are capable of phosphorylating Smad2 protein. When ES cells were treated with recombinant activin or Nodal for 1 hour in serum-free medium, Smad2 protein was strongly phosphorylated (Fig. 5A). By contrast, neither BMP-4 nor TGFβ phosphorylated Smad2 protein in ES cells (Fig. 5A), indicating that the TGFβ signal cannot be integrated into ES cells, as suggested above. In addition, expression of *Lefty-1* and *Lefty-2*, known target genes of Nodal (Juan and Hamada, 2001), was upregulated by treatment with recombinant Nodal (supplementary material Fig. S4), indicating that Nodal signaling was transduced into the nucleus in ES cells, as reported for other cells.

We then examined the effects of TGFβ superfamily ligands on ES cell proliferation in serum-free medium. Exogenous 30 ng/ml activin increased ES cell propagation ratio by 85% and 20% on Days 3 and 7, respectively. Furthermore, 1 or 2 μg/ml Nodal increased the ES cell propagation ratio on both Days 3 and 7 (Fig. 5B-D). Although 30 ng/ml exogenous BMP-4 appeared to slightly enhance ES cell propagation on Day 3, BMP-4 inhibited ES cell proliferation on Day 7 (Fig. 5B-D). These results suggest that activin and Nodal promote ES cell proliferation in serum-free medium via the canonical signal.

Exogenous Nodal signaling does not affect the pluripotency of mES cells

We previously found that serum-free medium supplemented with KSR and ACTH can maintain proper cellular pluripotency (Ogawa et al., 2004). In order to examine whether the undifferentiated state of ES cells was maintained when they were clonally expanded in serum-free medium supplemented with exogenous activin or Nodal, we determined the expression of ES cell markers such as *Oct3/4* (Niwa et al., 2000; Niwa et al., 2002), *Nanog* (Chambers et al., 2003; Mitsui et al., 2003), *Sox2* (Yuan et al., 1995), *Zfp42/Rex1* (Rogers et al., 1991) and *Utf1* (Okuda et al., 1998). As shown in Fig. 6A, these pluripotent state-specific genes were strongly expressed in each ES cell. To further examine the pluripotency of ES cells

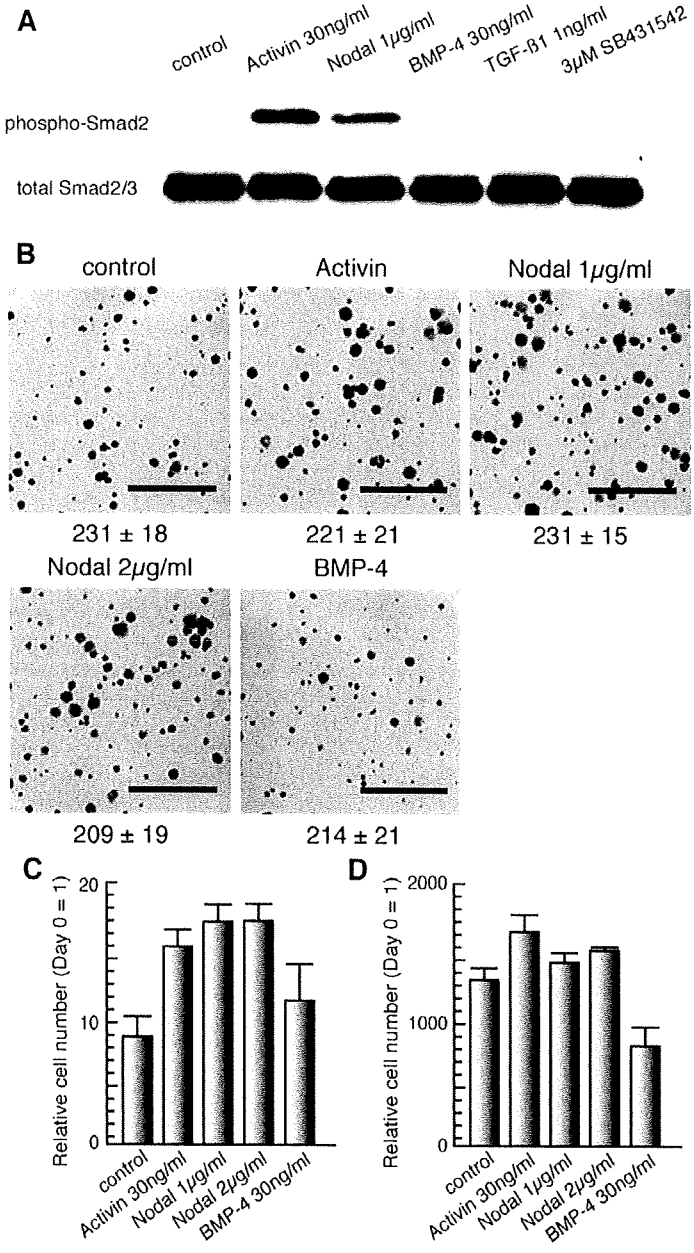

Fig. 5. Effects of TGFβ superfamily signaling on ES cell proliferation in serum-free conditions. (A) Effects of various TGFβ superfamily molecules on Smad2 phosphorylation in EB5 ES cells. EB5 cells were treated with the indicated factors for 1 hour, and subjected to western blot analysis using anti-phospho-Smad2 antibody (upper panel) and anti-Smad2/3 antibody (lower panel). (B) Colony morphologies of EB5 ES cells in serum-free medium supplemented with various TGFβ superfamily molecules. EB5 colonies were grown for 7 days in serum-free medium supplemented with no factor (as control), 30 ng/ml activin, 1 μg/ml Nodal, 2 μg/ml Nodal or 30 ng/ml BMP-4. Numbers indicate numbers of colonies appearing (n=3). Bars, 5 mm. (C,D) Relative numbers of cells treated with TGFβ superfamily molecules present on Day 3 (C) and Day 7 (D) of culture compared with that at Day 0. Each bar represents the mean ± s.e.m. (n=4).

treated with Nodal, we subcutaneously injected Nodal-treated ES cells into nude mice. These cells generated teratomas that grew to a few centimeters in size in 3-4 weeks. Histological examination revealed that they consisted of derivatives of all three germ layers, including hair-follicle-like structures with keratohyaline granules (ectoderm), cartilage (mesoderm), and ciliated or mucus-producing epithelia (endoderm) (Fig. 6B). Moreover, these cells produced overt chimeras with ES-derived agouti-chinchilla coat color (Fig. 6C). These results suggest that activin and Nodal enhance mES cell proliferation without affecting their pluripotency.

mES cells produces activin-Nodal activities for self-propagation

Although the growth-stimulatory activity of Nodal and activin was detected in serum-free medium, it was weaker than the proliferative activity inhibited by overexpression of *Smad7* or addition of SB-431542 to FCS-containing medium. To test for the presence of autocrine activin-Nodal activity, which might mask the effect of exogenous Nodal on ES cell proliferation, we performed luciferase reporter assay in serum-free medium without activin-Nodal supplementation. The relative activity of Id-1-luc was dramatically reduced in serum-free medium compared with that in FCS-containing medium (Fig. 7A). By contrast, removal of FCS resulted in the reduction of ARE-luc activity, which is consistent with the observation that Smad7 overexpression was less effective in repressing proliferation in serum-free culture, although it was less than that of Id-luc activity (Fig. 7A). We next investigated the effect of SB-431542 on ES cell proliferation in serum-free medium. Addition of 3 μM SB-431542 inhibited ES cell proliferation, as assessed by colony staining, cell number and proliferation intensity (Fig. 7B-D). The difference in proliferation ratio between fSmad7-10$^+$ and fSmad7-10$^-$ cells was less in serum-free medium than in FCS-containing medium. These results indicate that activin-Nodal signaling is autonomously activated in ES cells in serum-free conditions, and that activin-Nodal activity produced by ES cells masks the effects of exogenous Nodal or activin. Furthermore, signaling by soluble TGFβ-related molecules in FCS, presumably activin-Nodal, might increase endogenous activin-Nodal activity in ES cells.

Discussion

In the present study, we demonstrated, to our knowledge for the first time, that Nodal and activin promote mES cell proliferation with maintenance of pluripotent state in serum-free conditions. The findings presented here strongly suggest a contribution of Nodal signaling to maintenance of rapid proliferation of mES cells.

Possible roles of activin-Nodal signaling in pluripotent cell propagation during early embryogenesis

Many homozygous mutations of *Nodal*-related genes in mice result in reduction of pluripotent cell propagation

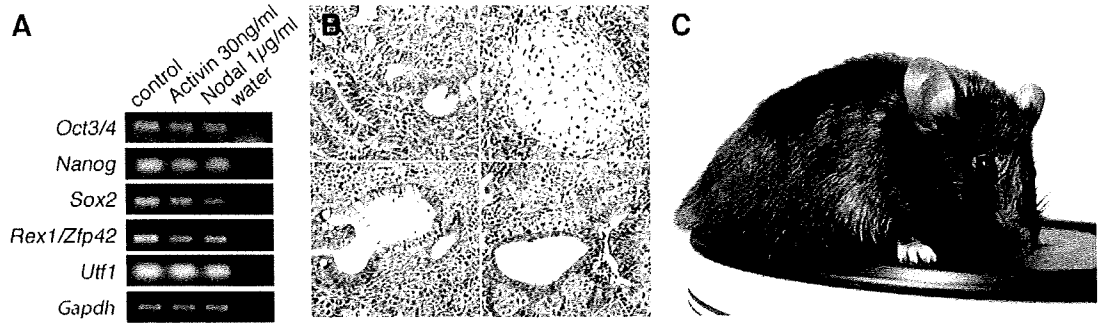

Fig. 6. Maintenance of undifferentiated state of ES cells cultured in serum-free medium with Nodal or activin. (A) Examination of expression of stem cell marker genes in EB5 ES cells clonally expanded and maintained for at least 1 month in serum-free medium supplemented with either 30 ng/ml activin or 1 μg/ml Nodal by RT-PCR analysis. *Gapdh* was detected as a loading control. (B) Hematoxylin and eosin staining of teratomas derived from EB5 ES cells cultured with Nodal protein. Tissues derived from each of the three germ layers were formed. Neuroectoderm (ectoderm; top left), cartilage (mesoderm; top right), mucus-producing epithelium (endoderm; bottom left) and ciliated epithelium (endoderm; bottom right) were observed. (C) Chimeric mouse derived from EB3 ES cells cultured with 2 μg/ml Nodal.

in early embryogenesis. ICM outgrowth is markedly reduced in *Smad4*$^{-/-}$ blastocysts (Yang et al., 1998), and the size of the epiblast cell population is substantially reduced in *Nodal*$^{-/-}$ or proprotein convertases for Nodal, *Spc1*$^{-/-}$/*Spc4*$^{-/-}$ embryos (Conlon et al., 1994; Beck et al., 2002; Robertson et al., 2003). In *Smad2*$^{-/-}$ mutant embryos, *Oct3/4* expressing regions are diminished by 8.5 days post coitus (d.p.c.), suggesting that pluripotent epiblast cells are prematurely lost (Waldrip et al., 1998). In the peri-implantation stage of the mouse embryo, the proliferation of pluripotent stem cells is tightly regulated. In the blastocyst, pluripotent stem cells exhibit very slow proliferation, with a doubling time of 64-65 hours (Copp, 1978). However, their growth accelerates after implantation, and doubling time is shortened to 11-12 hours at embryonic day 5.5 (E5.5), 9-10 hours at E6.0 and 4-5 hours at E6.5 (Snow, 1977). In serum-free medium, mES cells exhibit very slow proliferation, as pluripotent cells in ICM, at the beginning of culture, but their growth accelerates after the formation of a small colony about 5 days later (Ogawa et al., 2004). Furthermore, since the doubling time of ES cells cultured in FCS-containing medium is about 12 hours, their physiological characteristics resemble those of the epiblast around E5.0, suggesting that growth stimulation of mES cells after the formation of a small colony might correspond to the event triggering rapid epiblast growth after implantation. Interestingly, in mouse embryos, high levels of *Smad7* expression are detected during pre- and postimplantation stages when the epiblast cells are slow growing and gradually decrease from E6.5 to E7.5 while epiblast cell proliferation accelerates (Zwijsen et al., 2000), although the function of *Smad7* in mouse development has not yet been reported. These findings, together with those of the present study, suggest that the dramatic changes that occur in the proliferation of pluripotent cells during implantation stages may be regulated by Nodal, as a positive regulator, and Smad7, as a negative regulator.

Autocrine and paracrine loops of activin-Nodal signaling in ES cells

Consistent with our findings, several lines of evidence have suggested that activin-Nodal signaling is autonomously activated in human and mouse ES cells. The transcriptome of undifferentiated and differentiated hES cells was characterized to elucidate the signaling networks that play a role in the maintenance of the unique characteristics of hES cells (Brandenberger et al., 2004). These authors speculate that Nodal signaling is activated in undifferentiated hES cells, because components of Nodal signals (human orthologs of *Cripto* and *FAST1*) and a target gene (a human ortholog of *Lefty2*) are highly expressed in undifferentiated hES cells. Furthermore, phosphorylation of Smad2/3, but not of Smad1/5, was observed in undifferentiated hES cells, and decreased upon their differentiation (James et al., 2005).

We found that activin-Nodal signaling is autonomously activated in serum-free-cultured mES cells (Fig. 7), suggesting that mES cells produce activin-Nodal ligands, as supported by supplementary material Fig. S3. Notably, the target genes of Nodal include its positive regulators, such as the *Nodal* gene itself, and its negative regulators, such as *Lefty1* and *Lefty2* (Hamada et al., 2002). We failed to observe any effects of exogenous Nodal on proliferation of serum-free cultured ES cells when these cells were grown to confluence (data not shown), suggesting that Nodal ligands and/or Lefty1 and Lefty2 produced by autocrine loops of Nodal signaling in ES cells might mask the effects of exogenous Nodal or activin.

Roles of TGFβ superfamily signaling in self-renewal of ES cells

We found that exogenous addition of Nodal or activin increased mouse ES cell proliferation, whereas addition of BMP or TGFβ had no significant effects (Fig. 5B-D). The finding that TGFβ failed to affect ES cell proliferation can be explained by the lack of expression of type II receptors for TGFβ (supplementary material Fig. S3). By contrast, the failure of exogenous BMP-4 to stimulate proliferation of mES cells is inconsistent with previous reports (Ying et al., 2003a; Qi et al., 2004). BMP sustains self-renewal of mES cells in concert with LIF, and the crucial contribution of BMP to mES cell self-renewal is to induce expression of *Id* genes (Ying et al., 2003a). In N2B27 medium, which these authors used to

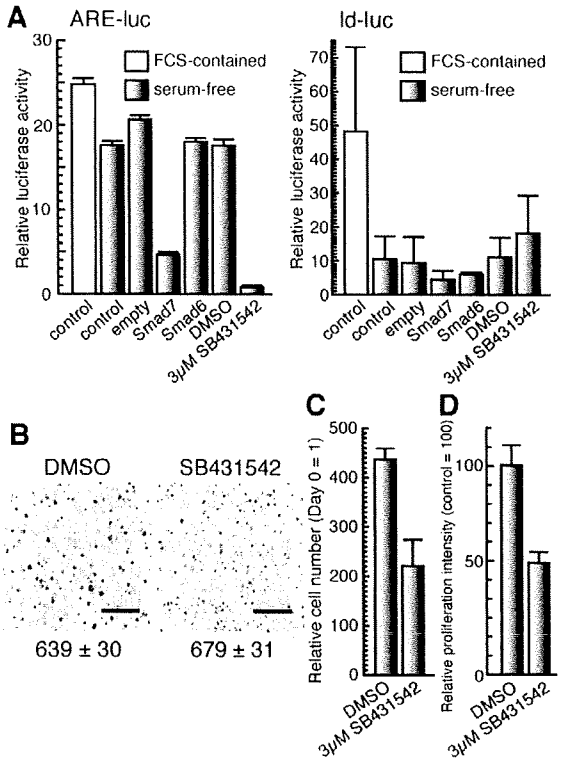

Fig. 7. ES cells produce activin-Nodal activities for self-propagation. (A) Luciferase reporter assay of MGZ5 cells with reporter constructs (ARE-luc reporter or Id-1-luc reporter). Control, cells transfected with reporter and control vectors only; Smad7, Smad6, empty, cells transfected with each expression plasmid; SB-431542, DMSO, cells cultured in medium supplemented with SB-431542 or DMSO (as control for SB-431542). Each bar represents the mean ± s.e.m. (n=3). (B) Colony morphologies of MGZ5 cells treated with SB-431542. MGZ5 cells were seeded at 2000 cells/well in six-well plates and cultured in serum-free medium supplemented with 3 μM SB-431542 (right) or DMSO (as control, left) for 1 week. Numbers indicate numbers of colonies appearing (n=3). Bars, 5 mm. (C) Relative numbers of cells treated with SB-431542 or DMSO present on Day 7 of culture compared with that at Day 0. Each bar represents the mean ± s.e.m. (n=3). (D) Relative proliferation intensity is shown as total cell number/number of colonies appearing, compared with that in cells treated with DMSO (100%). Each bar represents the mean ± s.e.m. (n=3).

test the effects of BMP, mES cells tend to differentiate into neural precursors and exhibit decreased proliferation even in the presence of LIF (Ying et al., 2003b). An autocrine BMP loop has been described in mES cells (Monteiro et al., 2004) and BMP provided by feeder cells has also been identified as a factor required for the maintenance of ES cell self-renewal (Qi et al., 2004). Since embryoid body formation studies have shown that BMP-4 inhibits neural differentiation, as found in many other vertebrate models (Wilson et al., 1995; Finley et al., 1999; Wilson and Edlund, 2001), the growth-stimulatory effects of BMP in the study by Ying et al. (Ying et al., 2003a) might have been due to its inhibitory effects on neural differentiation of mES cells intrinsically induced in serum-free conditions with N2B27 medium, in which B27 supplement contains vitamin A, a precursor of a potent differentiation inducer retinoic acid. By contrast, our serum-free culture conditions allow mES cells to maintain an undifferentiated state in the presence of LIF (Ogawa et al., 2004). To examine the possibility that endogenously activated BMP signals in our culture condition might have masked the effects of exogenous BMP-4 on mES cell proliferation, we studied the levels of Smad1/5/8 phosphorylation in the absence and presence of Noggin and BMP-4 (supplementary material Fig. S5A). Endogenous phosphorylation of Smad1/5/8 was barely detected whereas BMP-4 significantly induced their phosphorylation. While Noggin decreased Smad1/5/8 phosphorylation induced by BMP-4, it did not change the basal level of Smad1/5/8 phosphorylation, nor inhibit the mES cell propagation (supplementary material Fig. S5), suggesting that endogenous BMP signals did not play important roles under our culture conditions. We suspect that this is the reason why the present study, which focused on the effects of TGFβ superfamily members on the proliferation of undifferentiated mES cells, failed to detect growth-stimulatory effects of BMPs.

There is evidence that, during early embryogenesis, Nodal signaling plays a role in patterning of the anteroposterior body axis, formation of mesoderm and endoderm, and left-right axis patterning (Schier and Shen, 2000; Brennan et al., 2002; Eimon and Harland, 2002; Nonaka et al., 2002), suggesting that Nodal signaling induces cellular differentiation. Finding that the expression of *Zfp42/Rex-1* in Smad7-10 ES cells was higher than that in Smad7-10-1 and EB3 (supplementary material Fig. S2) suggests that endogenous activin-Nodal-TGFβ signaling might also be involved in the promotion of differentiation to primitive ectoderm of mES cells. However, in human ES cells, Nodal or activin-Nodal-TGFβ signaling plays a role in the inhibition of ES cell differentiation (Vallier et al., 2004; James et al., 2005; Beattie et al., 2005). Although addition of activin or Nodal to our serum-free medium in the absence of LIF did not significantly induce differentiation of mES cells (data not shown), it remains to be determined whether the growth-stimulatory activity of activin-Nodal signaling is associated with its potential to inhibit differentiation of mES cells.

How does Nodal signaling regulate growth and self-renewal of ES cells?

TGFβs have been shown to inhibit proliferation of many types of cells through upregulation of cell-cycle inhibitors, such as p21, p27, and p15 (Massague et al., 2000). Recently, Nodal was also shown to inhibit proliferation and induce apoptosis of human trophoblast cells through ALK7 and Smad2/3 (Munir et al., 2004). Therefore, our finding that Nodal enhances proliferation of ES cells seems exceptional. However, during formation of the anteroposterior body axis of mouse embryos, Nodal signaling provides the driving force for distal visceral endoderm (DVE) migration by stimulating the proliferation of visceral endodermal cells (Yamamoto et al., 2004), suggesting that Nodal is capable of enhancing the proliferation of certain types of cells.

To further investigate how Nodal promotes ES cell growth, we studied its effects on cell-cycle distribution and apoptosis. While activin did not affect the apoptosis of ES cells, addition of activin to ES cell culture resulted in a slight decrease in G1 ratio and subsequent increase in G2-M ratios (supplementary

material Fig. S6). The overall distribution of mES cells at different cell-cycle stages was not dramatically affected, suggesting that Nodal signaling may positively regulate the cell cycle. We examined whether the stimulation of activin or Nodal might influence the expression of *ERas*, *Utf1*, *B-Myb*, *Myc* and *CDK4*, which are reported to be components involved in propagation of mouse ES cells (Savatier et al., 1996; Iwai et al., 2001; Takahashi et al., 2003; Cartwright et al., 2005; Nishimoto et al., 2005). We found that both Nodal and activin induced a significant increase in the expression of *ERas* and *Utf1*, whereas they induced a decrease in *B-Myb* expression (supplementary material Fig. S7). Clarification of the mechanisms whereby exogenous activin-Nodal signaling regulates the propagation of mouse ES cells will require further biochemical analyses using activin- or Nodal-null ES cells in which autocrine loops of activin-Nodal signal are absent.

Various signaling cascades, such as LIF-STAT3 (Smith et al., 1988; Niwa et al., 1998; Matsuda et al., 1999) and Wnt (Sato et al., 2004; Ogawa et al., 2006), and transcription factors, such as Oct3/4 (Niwa et al., 2000; Niwa et al., 2002; Niwa et al., 2005) and Nanog (Chambers et al., 2003; Mitsui et al., 2003), are thought to play roles in the maintenance of self-renewal and/or pluripotency of ES cells. Further investigation is needed to determine the molecular mechanisms by which activin-Nodal signaling cooperates with such signaling or transcriptional networks to regulate ES cell proliferation.

We previously reported that ES cells produce an activity to support their clonal propagation in serum-free medium (Ogawa et al., 2004). Stem cell colonies were never formed from single cells in low-density culture (<100 cells/cm^2) in medium supplemented with 10% KSR and 1000 U/ml LIF (KSR medium). However, addition of a small amount (0.3%) of the final volume of FCS or 1-10 μM ACTH to KSR medium caused clonal ES cell propagation. We therefore hypothesized that a factor possessing ACTH-like activity is secreted by ES cell themselves, which we designated stem-cell autocrine factor (SAF). Since activin and Nodal enhance ES cell proliferation in an autocrine fashion, we questioned whether activin-Nodal activities mimic SAF activity. However, the addition of either activin or Nodal did not promote clonal propagation in KSR medium (data not shown), suggesting that at least two autocrine activities, those of SAF and activin-Nodal, support ES cell propagation in serum-free conditions. Based on our previous findings (Ogawa et al., 2004), we hypothesize that the survival of ES cells cultured in serum-free medium was supported by SAF activity at the start of culture, and that the growth of the attached ES cells is accelerated by upregulated autocrine Nodal signaling after cells have formed small colonies in low-density culture.

ES cells have attracted the interest of many researchers partly because of their promise for applications in regenerative medicine. However, such use requires that risks of pathogenic contamination caused by the addition of serum to medium be avoided. While the present findings obtained by mouse ES cells need to be carefully examined to be applicable for human ES cells, we hope that the combination of previously determined serum-free culture conditions and use of recombinant activin and/or Nodal will yield a safe and efficient protocol for propagation of ES cells in a completely chemically defined medium.

Materials and Methods

ES cell culture and supertransfection

MGZ5 (derived from CCE), EB5 and EB3 (derived from E14tg2a) ES cells were maintained on feeder-free, gelatin-coated plates in LIF-supplemented medium as described previously (Niwa et al., 2002). Serum-free culture medium with knockout serum replacement (KSR, Invitrogen) and 10 μM adrenocorticotrophic hormone (ACTH; American Peptides) was described previously (Ogawa et al., 2004). To assess the clonal propagation of ES cells, EB5 cells were seeded at 300 cells/well in 12-well plates and cultured in serum-free medium supplemented with various growth factors. SB-431542 (Sigma) was prepared as previously described (Watabe et al., 2003). BMP-4 (30 ng/ml), TGFβ1 (1 ng/ml), activin (30 ng/ml), Nodal (1 or 2 μg/ml) and Noggin (90 ng/ml) were purchased from R&D Systems and used in each experiment at these concentrations unless specifically noted otherwise. The colonies that appeared were stained with Leishman's reagent (Sigma) or BCIP/NBT solution (Sigma) for alkaline phosphatase staining. Transfection of episomal expression vectors [pCAG-IRESpuropA (pCAG-IP)] into MGZ5 cells (supertransfection) was performed using Lipofectamine 2000 (Invitrogen) as described previously (Niwa et al., 2002).

Generation of fSmad7-10+ and fSmad7-10- ES cells

pCAG-floxed-*DsRed*-IRES*pacEGFP* expression vector was constructed by ligation of loxP fragment, Discosoma red fluorescent protein (*DsRed*) *T4* (Bevis and Glick, 2002) expression cassette derived from pBluescript SK$^-$*DsRed T4*, and enhanced green fluorescent protein (*EGFP*) expression cassette derived from pEGFP (Clontech) into pCAG-IP. *Smad7* cDNA was introduced into the *Xho*I and *Not*I sites of pCAG-floxed-*DsRed*-IRES*pacEGFP* to obtain pCAG-f*Smad7*R-IRES*pacEGFP*.

In stable integration experiments, 2×10^7 EB3 ES cells were electroporated with 100 μg of linearized pCAG-f*Smad7*R-IRES*pacEGFP* DNA at 800 V and 3 μF in a 0.4-cm cuvette using a Gene Pulser II (Bio-Rad Laboratories) and cultured in the presence of 1 μg/ml puromycin. After 7-10 days, colonies were isolated for clonal expansion, and one of them, named fSmad7-10$^+$, was maintained in the presence of 1 μg/ml puromycin for 1 month. fSmad7-10$^-$ ES cells were generated by Cre recombination using pCAGGS-*Cre* and maintained in the presence of 1 μg/ml puromycin.

Luciferase reporter assay

MGZ5 cells were transiently transfected with an appropriate combination of reporter vector and expression plasmids together with *Renilla* luciferase control reporter vector (pTK-RL or pRL-CMV) using Lipofectamine 2000 (Invitrogen) as previously described (Chen et al., 1996; Yagi et al., 1999; Korchynskyi and ten Dijke, 2002; Kahata et al., 2004). Luciferase activities were normalized to the luciferase activity of co-transfected pTK-RL or pRL-CMV.

RNA isolation, northern blot and RT-PCR analysis

Total RNAs were prepared with ISOGEN reagent (Nippongene) or TRIzol reagent (Invitrogen) according to the manufacturer's instructions. Oligo(dT)-primed cDNAs were prepared from 1 μg of total RNA using SuperScript reverse transcriptase (Clontech) or ReverTra Ace (Toyobo). For northern blot analysis, 5 μg of total RNA were separated on a denaturing agarose gel, and then blotted onto Hybond-N membrane (Amersham Biosciences). Probes used for northern blot analyses have been previously described (Ogawa et al., 2004). Analysis was performed with GeneImage (Amersham Biosciences) according to the manufacturer's instructions. Expression of various signaling components was compared by RT-PCR analysis. PCR products were separated by electrophoresis in 1% agarose gel and visualized with ethidium bromide. Quantitative real-time RT-PCR analysis was performed using the GeneAmp 5700 Sequence Detection System (Applied Biosystems) or MyiQ Real-Time PCR Detection Systems (Bio-Rad Laboratories). Primer sequences used for PCR reactions are described in supplementary material Table S1.

Western blot analysis

Antibodies for phospho-Smad2, Smad2/3 and phospho-Smad1/5/8 for western blot analysis were obtained from Cell Signaling. Antibodies for α-tubulin were obtained from Sigma. Western blot analysis was performed as described (Kawabata et al., 1998).

Teratoma formation and generation of chimeric mouse

EB5 cells were cultured in serum-free medium supplemented with Nodal protein at clonal density for two weeks. Cells suspended in phosphate-buffered saline were subcutaneously injected into the flank of nude mice. After 3 weeks, the teratomas were excised, fixed in 10% paraformaldehyde, and subjected to histological examination with hematoxylin and eosin staining. fSmad 7-10$^-$ cells were cultured in medium supplemented with 1 μg/ml puromycin for more than 1 month. EB3 cells were cultured in serum-free medium supplemented with 2 μM recombinant Nodal at clonal density for more than 1 month. Microinjection of fSmad7-10$^-$ and EB3 ES cells into C57BL/6J blastocysts was performed according to standard procedures (Hogan et al., 1994).

Cell-cycle analysis

EB5 cells were stimulated with 30 ng/ml Activin for 24 hours. All cells (attached and detached) were collected, washed once in PBS, and the cellular DNA was stained with propidium iodide (25 μg/ml; Sigma). The cellular DNA content was analyzed by FACS (Beckman Coulter, Fullerton, CA).

We thank R. Watanabe (Kyoto University) for providing mouse *Smad6* and *Smad7* cDNAs, Tetsutaro Hayashi (RIKEN, CDB) for technical support of FACS analyses and Arisa Mita (University of Tokyo) for technical support of teratoma formation assays. This work was supported in part by a Grant Aid for Scientific Research from the Ministry of Education, Science, Culture of Japan award (to H.N. and K.M.), and Leading Project (to H.N.).

References

Beattie, G. M., Lopez, A. D., Bucay, N., Hinton, A., Firpo, M. T., King, C. C. and Hayek, A. (2005). Activin a maintains pluripotency of human embryonic stem cells in the absence of feeder layers. *Stem Cells* **23**, 489-495.

Beck, S., Le Good, J. A., Guzman, M., Ben Haim, N., Roy, K., Beermann, F. and Constam, D. B. (2002). Extraembryonic proteases regulate Nodal signalling during gastrulation. *Nat. Cell Biol.* **4**, 981-985.

Bevis, B. J. and Glick, B. S. (2002). Rapidly maturing variants of the Discosoma red fluorescent protein (DsRed). *Nat. Biotechnol.* **20**, 83-87.

Brandenberger, R., Wei, H., Zhang, S., Lei, S., Murage, J., Fisk, G. J., Li, Y., Xu, C., Fang, R., Guegler, K. et al. (2004). Transcriptome characterization elucidates signaling networks that control human ES cell growth and differentiation. *Nat. Biotechnol.* **22**, 707-716.

Brennan, J., Norris, D. P. and Robertson, E. J. (2002). Nodal activity in the node governs left-right asymmetry. *Genes Dev.* **16**, 2339-2344.

Cartwright, P., McLean, C., Sheppard, A., Rivett, D., Jones, K. and Dalton, S. (2005). LIF/STAT3 controls ES cell self-renewal and pluripotency by a Myc-dependent mechanism. *Development* **132**, 885-896.

Chambers, I., Colby, D., Robertson, M., Nichols, J., Lee, S., Tweedie, S. and Smith, A. (2003). Functional expression cloning of Nanog, a pluripotency sustaining factor in embryonic stem cells. *Cell* **113**, 643-655.

Chen, X., Rubock, M. J. and Whitman, M. (1996). A transcriptional partner for MAD proteins in TGF-beta signalling. *Nature* **383**, 691-696.

Conlon, F. L., Lyons, K. M., Takaesu, N., Barth, K. S., Kispert, A., Herrmann, B. and Robertson, E. J. (1994). A primary requirement for nodal in the formation and maintenance of the primitive streak in the mouse. *Development* **120**, 1919-1928.

Copp, A. J. (1978). Interaction between inner cell mass and trophectoderm of the mouse blastocyst. I. A study of cellular proliferation. *J. Embryol. Exp. Morphol.* **48**, 109-125.

Eimon, P. M. and Harland, R. M. (2002). Effects of heterodimerization and proteolytic processing on Derriere and Nodal activity: implications for mesoderm induction in Xenopus. *Development* **129**, 3089-3103.

Finley, M. F., Devata, S. and Huettner, J. E. (1999). BMP-4 inhibits neural differentiation of murine embryonic stem cells. *J. Neurobiol.* **40**, 271-287.

Goumans, M. J., Ward-van Oostwaard, D., Wianny, F., Savatier, P., Zwijsen, A. and Mummery, C. (1998). Mouse embryonic stem cells with aberrant transforming growth factor beta signalling exhibit impaired differentiation in vitro and in vivo. *Differentiation* **63**, 101-113.

Hamada, H., Meno, C., Watanabe, D. and Saijoh, Y. (2002). Establishment of vertebrate left-right asymmetry. *Nat. Rev. Genet.* **3**, 103-113.

Hanyu, A., Ishidou, Y., Ebisawa, T., Shimanuki, T., Imamura, T. and Miyazono, K. (2001). The N domain of Smad7 is essential for specific inhibition of transforming growth factor-beta signaling. *J. Cell Biol.* **155**, 1017-1027.

Hata, A., Lagna, G., Massague, J. and Hemmati-Brivanlou, A. (1998). Smad6 inhibits BMP/Smad1 signaling by specifically competing with the Smad4 tumor suppressor. *Genes Dev.* **12**, 186-197.

Heldin, C. H., Miyazono, K. and ten Dijke, P. (1997). TGF-beta signalling from cell membrane to nucleus through SMAD proteins. *Nature* **390**, 465-471.

Hogan, B., Beddington, R., Constantini, F. and Lacy, E. (1994). *Manipulating the Mouse Embryo.* Cold Spring Harbor, NY: Cold Spring Harbor Laboratory Press.

Imamura, T., Takase, M., Nishihara, A., Oeda, E., Hanai, J., Kawabata, M. and Miyazono, K. (1997). Smad6 inhibits signalling by the TGF-beta superfamily. *Nature* **389**, 622-626.

Inman, G. J., Nicolas, F. J., Callahan, J. F., Harling, J. D., Gaster, L. M., Reith, A. D., Laping, N. J. and Hill, C. S. (2002). SB-431542 is a potent and specific inhibitor of transforming growth factor-beta superfamily type I activin receptor-like kinase (ALK) receptors ALK4, ALK5, and ALK7. *Mol. Pharmacol.* **62**, 65-74.

Itoh, S., Landstrom, M., Hermansson, A., Itoh, F., Heldin, C. H., Heldin, N. E. and ten Dijke, P. (1998). Transforming growth factor beta1 induces nuclear export of inhibitory Smad7. *J. Biol. Chem.* **273**, 29195-29201.

Ivanova, N. B., Dimos, J. T., Schaniel, C., Hackney, J. A., Moore, K. A. and Lemischka, I. R. (2002). A stem cell molecular signature. *Science* **298**, 601-604.

Iwai, N., Kitajima, K., Sakai, K., Kimura, T. and Nakano, T. (2001). Alteration of cell adhesion and cell cycle properties of ES cells by an inducible dominant interfering Myb mutant. *Oncogene* **20**, 1425-1434.

James, D., Levine, A. J., Besser, D. and Hemmati-Brivanlou, A. (2005). TGFß/activin/nodal signaling is necessary for the maintenance of pluripotency in human embryonic stem cells. *Development* **132**, 1273-1282.

Juan, H. and Hamada, H. (2001). Roles of nodal-lefty regulatory loops in embryonic patterning of vertebrates. *Genes Cells* **6**, 923-930.

Kahata, K., Hayashi, M., Asaka, M., Hellman, U., Kitagawa, H., Yanagisawa, J., Kato, S., Imamura, T. and Miyazono, K. (2004). Regulation of transforming growth factor-beta and bone morphogenetic protein signalling by transcriptional coactivator GCN5. *Genes Cells* **9**, 143-151.

Kawabata, M., Inoue, H., Hanyu, A., Imamura, T. and Miyazono, K. (1998). Smad proteins exist as monomers in vivo and undergo homo- and hetero-oligomerization upon activation by serine/threonine kinase receptors. *EMBO J.* **17**, 4056-4065.

Korchynskyi, O. and ten Dijke, P. (2002). Identification and functional characterization of distinct critically important bone morphogenetic protein-specific response elements in the Id1 promoter. *J. Biol. Chem.* **277**, 4883-4891.

Laping, N. J., Grygielko, E., Mathur, A., Butter, S., Bomberger, J., Tweed, C., Martin, W., Fornwald, J., Lehr, R., Harling, J. et al. (2002). Inhibition of transforming growth factor (TGF)-beta1-induced extracellular matrix with a novel inhibitor of the TGF-beta type I receptor kinase activity: SB-431542. *Mol. Pharmacol.* **62**, 58-64.

Massague, J. (1998). TGF-beta signal transduction. *Annu. Rev. Biochem.* **67**, 753-791.

Massague, J., Blain, S. W. and Lo, R. S. (2000). TGFbeta signaling in growth control, cancer, and heritable disorders. *Cell* **103**, 295-309.

Matsuda, T., Nakamura, T., Nakao, K., Arai, T., Katsuki, M., Heike, T. and Yokota, T. (1999). STAT3 activation is sufficient to maintain an undifferentiated state of mouse embryonic stem cells. *EMBO J.* **18**, 4261-4269.

Mitsui, K., Tokuzawa, Y., Itoh, H., Segawa, K., Murakami, M., Takahashi, K., Maruyama, M., Maeda, M. and Yamanaka, S. (2003). The homeoprotein Nanog is required for maintenance of pluripotency in mouse epiblast and ES cells. *Cell* **113**, 631-642.

Monteiro, R. M., de Sousa Lopes, S. M., Korchynskyi, O., ten Dijke, P. and Mummery, C. L. (2004). Spatio-temporal activation of Smad1 and Smad5 in vivo: monitoring transcriptional activity of Smad proteins. *J. Cell Sci.* **117**, 4653-4663.

Munir, S., Xu, G., Wu, Y., Yang, B., Lala, P. K. and Peng, C. (2004). Nodal and ALK7 inhibit proliferation and induce apoptosis in human trophoblast cells. *J. Biol. Chem.* **279**, 31277-31286.

Nakao, A., Afrakhte, M., Moren, A., Nakayama, T., Christian, J. L., Heuchel, R., Itoh, S., Kawabata, M., Heldin, N. E., Heldin, C. H. et al. (1997). Identification of Smad7, a TGFbeta-inducible antagonist of TGF-beta signalling. *Nature* **389**, 631-635.

Nishimoto, M., Miyagi, S., Yamagishi, T., Sakaguchi, T., Niwa, H., Muramatsu, M. and Okuda, A. (2005). Oct-3/4 maintains the proliferative embryonic stem cell state via specific binding to a variant octamer sequence in the regulatory region of the UTF1 locus. *Mol. Cell. Biol.* **25**, 5084-5094.

Niwa, H. (2001). Molecular mechanism to maintain stem cell renewal of ES cells. *Cell Struct. Funct.* **26**, 137-148.

Niwa, H., Burdon, T., Chambers, I. and Smith A. (1998). Self-renewal of pluripotent embryonic stem cells is mediated via activation of STAT3. *Genes Dev.* **12**, 2048-2060.

Niwa, H., Miyazaki, J. and Smith, A. G. (2000). Quantitative expression of Oct-3/4 defines differentiation, dedifferentiation or self-renewal of ES cells. *Nat. Genet.* **24**, 372-376.

Niwa, H., Masui, S., Chambers, I., Smith, A. G. and Miyazaki, J. (2002). Phenotypic complementation establishes requirements for specific POU domain and generic transactivation function of Oct-3/4 in embryonic stem cells. *Mol. Cell. Biol.* **22**, 1526-1536.

Niwa, H., Toyooka, Y., Shimosato, D., Strumpf, D., Takahashi, K., Yagi, R. and Rossant, J. (2005). Interaction between Oct3/4 and Cdx2 determines trophectoderm differentiation. *Cell* **123**, 917-929.

Nonaka, S., Shiratori, H., Saijoh, Y. and Hamada, H. (2002). Determination of left-right patterning of the mouse embryo by artificial nodal flow. *Nature* **418**, 96-99.

Ogawa, K., Matsui, H., Ohtsuka, S. and Niwa, H. (2004). A novel mechanism for regulating clonal propagation of mouse ES cells. *Genes Cells* **9**, 471-477.

Ogawa, K., Nishinakamura, R., Iwamatsu,Y., Shimosato, D. and Niwa, H. (2006). Synergistic action of Wnt and LIF in maintaining pluripotency of mouse ES cells. *Biochem. Biophys. Res. Commun.* **343**, 159-166.

Okuda, A., Fukushima, A., Nishimoto, M., Orimo, A., Yamagishi, T., Nabeshima, Y., Kuro-o, M., Boon, K., Keaveney, M., Stunnenberg, H. G. et al. (1998). UTF1, a novel transcriptional coactivator expressed in pluripotent embryonic stem cells and extra-embryonic cells. *EMBO J.* **17**, 2019-2032.

Qi, X., Li, T. G., Hao, J., Hu, J., Wang, J., Simmons, H., Miura, S., Mishina, Y. and Zhao, G. Q. (2004). BMP4 supports self-renewal of embryonic stem cells by inhibiting mitogen-activated protein kinase pathways. *Proc. Natl. Acad. Sci. USA* **101**, 6027-6032.

Ramalho-Santos, M., Yoon, S., Matsuzaki, Y., Mulligan, R. C. and Melton, D. A. (2002). "Stemness": transcriptional profiling of embryonic and adult stem cells. *Science* **298**, 597-600.

Raz, R., Lee, C. K., Cannizzaro, L. A., d'Eustachio, P. and Levy, D. E. (1999). Essential role of STAT3 for embryonic stem cell pluripotency. *Proc. Natl. Acad. Sci. USA* **96**, 2846-2851.

Robertson, E. J., Norris, D. P., Brennan, J. and Bikoff, E. K. (2003). Control of early anterior-posterior patterning in the mouse embryo by TGF-beta signalling. *Philos. Trans. R. Soc. Lond. B Biol. Sci.* **358**, 1351-1357.

Rogers, M. B., Hosler, B. A. and Gudas, L. J. (1991). Specific expression of a retinoic acid-regulated, zinc-finger gene, Rex-1, in preimplantation embryos, trophoblast and spermatocytes. *Development* **113**, 815-824.

Sato, N., Meijer, L., Skaltsounis, L., Greengard, P. and Brivanlou, A. H. (2004). Maintenance of pluripotency in human and mouse embryonic stem cells through activation of Wnt signaling by a pharmacological GSK-3-specific inhibitor. *Nat. Med.* **10**, 55-63.

Savatier, P., Lapillonne, H., van Grunsven, L. A., Rudkin, B. B. and Samarut, J. (1996). Withdrawal of differentiation inhibitory activity/leukemia inhibitory factor up-regulates D-type cyclins and cyclin-dependent kinase inhibitors in mouse embryonic stem cells. *Oncogene* **12**, 309-322.

Schier, A. F. and Shen, M. M. (2000). Nodal signalling in vertebrate development. *Nature* **403**, 385-389.

Schofield, R. (1978). The relationship between the spleen colony-forming cell and the haemopoietic stem cell. *Blood Cells* **4**, 7-25.

Sirard, C., de la Pompa, J. L., Elia, A., Itie, A., Mirtsos, C., Cheung, A., Hahn, S., Wakeham, A., Schwartz, L., Kern, S. E. et al. (1998). The tumor suppressor gene Smad4/Dpc4 is required for gastrulation and later for anterior development of the mouse embryo. *Genes Dev.* **12**, 107-119.

Smith, A. G., Heath, J. K., Donaldson, D. D., Wong, G. G., Moreau, J., Stahl, M. and Rogers, D. (1988). Inhibition of pluripotential embryonic stem cell differentiation by purified polypeptides. *Nature* **336**, 688-690.

Snow, M. H. L. (1977). Gastrulation in the mouse: growth and regionalization of epiblast. *J. Embryol. Exp. Morphol.* **42**, 293-303.

Takahashi, K., Mitsui, K. and Yamanaka, S. (2003). Role of ERas in promoting tumour-like properties in mouse embryonic stem cells. *Nature* **423**, 541-545.

Vallier, L., Reynolds, D. and Pedersen, R. A. (2004). Nodal inhibits differentiation of human embryonic stem cells along the neuroectodermal default pathway. *Dev. Biol.* **275**, 403-421

Viswanathan, S., Benatar, T., Rose-John, S., Lauffenburger, D. A. and Zandstra, P. W. (2002). Ligand/receptor signaling threshold (LIST) model accounts for gp130-mediated embryonic stem cell self-renewal responses to LIF and HIL-6. *Stem Cells* **20**, 119-138.

Waldrip, W. R, Bikoff, E. K., Hoodless, P. A., Wrana, J. L. and Robertson, E. J. (1998). Smad2 signaling in extraembryonic tissues determines anterior-posterior polarity of the early mouse embryo. *Cell* **92**, 797-808.

Watabe, T., Nishihara, A., Mishima, K., Yamashita, J., Shimizu, K., Miyazawa, K., Nishikawa, S. and Miyazono, K. (2003). TGF-beta receptor kinase inhibitor enhances growth and integrity of embryonic stem cell-derived endothelial cells. *J. Cell Biol.* **163**, 1303-1311.

Wilson, P. A. and Hemmati-Brivanlou, A. (1995). Induction of epidermis and inhibition of neural fate by Bmp-4. *Nature* **376**, 331-333.

Wilson, S. I. and Edlund, T. (2001). Neural induction: toward a unifying mechanism. *Nat. Neurosci.* **4**, 1161-1168.

Yagi, K., Goto, D., Hamamoto, T., Takenoshita, S., Kato, M. and Miyazono, K. (1999). Alternatively spliced variant of Smad2 lacking exon 3. Comparison with wild-type Smad2 and Smad3. *J. Biol. Chem.* **274**, 703-709.

Yamamoto, M., Saijoh, Y., Perea-Gomez, A., Shawlot, W., Behringer, R. R., Ang, S. L., Hamada, H. and Meno, C. (2004). Nodal antagonists regulate formation of the anteroposterior axis of the mouse embryo. *Nature* **428**, 387-392.

Yan, Y. T., Liu, J. J., Luo, Y., Chaosu, E., Haltiwanger, R. S., Abate-Shen, C. and Shen, M. M. (2002). Dual roles of Cripto as a ligand and coreceptor in the nodal signaling pathway. *Mol. Cell. Biol.* **22**, 4439-4449.

Yang, X., Li, C., Xu, X., and Deng, C. (1998). The tumor suppressor SMAD4/DPC4 is essential for epiblast proliferation and mesoderm induction in mice. *Proc. Natl. Acad. Sci. USA* **96**, 3667-3672.

Ying, Q. L., Nichols, J., Chambers, I. and Smith, A. (2003a). BMP induction of Id proteins suppresses differentiation and sustains embryonic stem cell self-renewal in collaboration with STAT3. *Cell* **115**, 281-292.

Ying, Q. L., Stavridis, M., Griffiths, D., Li, M. and Smith, A. (2003b). Conversion of embryonic stem cells into neuroectodermal precursors in adherent monoculture. *Nat. Biotechnol.* **21**, 183-186.

Yuan, H., Corbi, N., Basilico, C. and Dailey, L. (1995). Developmental-specific activity of the FGF-4 enhancer requires the synergistic action of Sox2 and Oct-3. *Genes Dev.* **9**, 2635-2645.

Zwijsen, A., van Rooijen, M. A., Goumans, M. J., Dewulf, N., Bosman, E. A., ten Dijke, P., Mummery, C. L. and Huylebroeck, D. (2000). Expression of the inhibitory Smad7 in early mouse development and upregulation during embryonic vasculogenesis. *Dev. Dyn.* **218**, 663-670.

Journal of Cell Science

Editorial

VEGFR1 for Lymphangiogenesis
An Alternative Signaling Pathway?

Yasufumi Sato

The lymphatic vascular system is a conduit for interstitial fluid extravasated from blood vessels and also plays important roles in maintaining immune responses, lipid uptake, and tissue homeostasis. In recent years, much attention has been given to lymphangiogenesis, a formation of new lymphatic vessels, because lymphangiogenesis has been shown to be involved in lymph node metastasis of tumors.[1]

See accompanying article on page 658

The development of blood and lymphatic vascular systems is primarily regulated by vascular endothelial growth factor (VEGF) family members. This family consists of 5 members: VEGF-A, VEGF-B, VEGF-C, VEGF-D, and placenta growth factor (PlGF). There are 3 members of VEGF receptor (VEGFR) tyrosine kinases: VEGFR1, VEGFR2, and VEGFR3. Members of the VEGF family show different affinities for these receptors. VEGFR1 is able to bind VEGF-A, VEGF-B, and PlGF. VEGFR2 is activated primarily by VEGF-A, but cleaved forms of VEGF-C and VEGF-D may also activate this receptor. VEGFR3 is activated by VEGF-C and VEGF-D. Vascular endothelial cells (ECs) express VEGFR1 and VEGFR2, whereas lymphatic ECs express VEGFR2 and VEGFR3 in the adult. The most important molecule in the VEGF family that controls angiogenesis is VEGF-A, and VEGFR2 is the major mediator of VEGF-A driven responses in vascular ECs. VEGFR1, on the other hand, has a higher affinity for VEGF-A but weaker tyrosine kinase activity. Thus, VEGFR1 on vascular ECs may act as a counter-regulator of VEGFR2. VEGFR1 is also expressed by monocytes/macrophages and hematopoietic stem cells, and in those cases, VEGFR1 transduces signal for the migration of those cells. Therefore, VEGFR-1 has a dual function, acting in a positive or negative manner in different cell types or circumstances. The most important molecule in the VEGF family that controls lymphangiogenesis are VEGF-C and VEGF-D, and VEGFR3 is the major mediator of VEGF-C and VEGF-D driven responses in lymphatic ECs. However, VEGF-A may stimulate VEGFR2 on lymphatic ECs and induce lymphangiogenesis directly.[2]

The induction of VEGF-A is important for the initiation of angiogenesis. The principal trigger of angiogenesis is hypoxia, which induces the expression VEGF-A in various cell types. This induction in hypoxia is mediated by a transcription factor known as hypoxia-inducible factor 1 (HIF-1), a heterodimeric complex of HIF-1α and HIF-1β subunits, which binds to hypoxia responsive element (HRE) in the promoter of VEGF-A gene. Under normal oxygen tension, the expression of VEGF-A is suppressed by the product of a tumor suppressor gene known as the von Hippel Lindau (VHL) gene, which is involved in the degradation of HIF-1α through the ubiquitin proteasome system.[2] Angiogenesis is normally associated with, or followed by, lymphangiogenesis, because defective lymphangiogenesis should cause tissue edema. However, little is known about the trigger of lymphangiogenesis. The aberrant expression of VEGF-C or VEGF-D and its correlation with lymph node metastasis was described in various tumors.[1] Nevertheless, only a few studies have focused on the regulation of the expression of VEGF-C or VEGF-D. A transcription factor known as nuclear factor-kappa B (NF-κB) or an enzyme known as cycloxygenase-2 (COX-2) is involved in the upregulation of VEGF-C in certain cancer cells.[3–5]

In this issue of *Arteriosclerosis, Thrombosis, and Vascular Biology*, Murakami et al propose that the signal via VEGFR1 promotes angiogenesis in parallel with lymphangiogenesis through the recruitment of macrophages. To test the function of VEGFR1, they use K14 *Vefg-A* Tg mice, *Vegfr1* $tk^{-/-}$ mice, and a double mutant of K14 *Vefg-A* Tg *Vegfr1* $tk^{-/-}$ mice. K14 *Vefg-A* Tg *Vegfr1* $tk^{-/-}$ mice show a significant decrease in angiogenesis and lymphangiogenesis in subcutaneous tissue where VEGF-A is overexpressed. To address the mechanism underlying this decrease of angiogenesis and lymphangiogenesis in K14 *Vefg-A* Tg *Vegfr1* $tk^{-/-}$ mice, they focus on the recruitment of macrophages into subcutaneous tissue. VEGF-A augments the recruitment of macrophages through the activation of VEGFR1 on macrophages. This recruitment of macrophages is reduced in K14 *Vefg-A* Tg *Vegfr1* $tk^{-/-}$ mice. Moreover, K14 *Vefg-A* Tg mice that receive bone marrow transplantation from *Vegfr1* $tk^{-/-}$ mice show the reduction of macrophage recruitment as well as the decrease of angiogenesis and lymphangiogenesis. Thus, they conclude that VEGF-A stimulates mobilization and recruitment of macrophages from bone marrow through VEGFR1, and that is required for angiogenesis and lymphangiogenesis.

The role of macrophage recruitment in angiogenesis has been well documented.[6] In addition, several recent articles described the involvement of macrophage recruitment in lymphangiogenesis as well. Schoppmann et al showed that, in certain human cancers, the density of lymphatic microvessels was significantly increased in peritumoral stroma, and that a subset of cells in peritumoral stroma, namely tumor-

From the Department of Vascular Biology, Institute of Development, Aging, and Cancer, Tohoku University, Japan.

Correspondence to Yasufumi Sato, Department of Vascular Biology, Institute of Development, Aging, and Cancer, Tohoku University, 4-1 Seiryo-machi, Aoba-ku, Sendai 980-8575, Japan. E-mail y-sato@idac.tohoku.ac.jp

(*Arterioscler Thromb Vasc Biol.* 2008;28:604-605.)

Arterioscler Thromb Vasc Biol is available at http://atvb.ahajournals.org
DOI: 10.1161/ATVBAHA.108.162032

associated macrophages (TAMs), expressed VEGF-C and VEGF-D. Their data indicated that the density of TAMs producing VEGF-C and VEGF-D correlated with peritumoral inflammatory reaction, peritumoral lymphangiogenesis, and frequency of lymph node metastasis.[7,8] Cursiefen et al reported the relationship between VEGF-A stimulated lymphangiogenesis and macrophage recruitment in the suture-induced inflammatory corneal model of mice. Administration of VEGF Trap, a receptor-based fusion protein that neutralized VEGF-A but not VEGF-C or VEGF-D, completely inhibited both angiogenesis and lymphangiogenesis after corneal injury. Moreover, either systemic depletion of bone marrow–derived cells by irradiation or local depletion of macrophages in the cornea by clodronate liposome significantly inhibited angiogenesis and lymphangiogenesis in the cornea.[9] Maruyama et al revealed that the decreased number of macrophages correlated with the reduced lymphangiogenesis in the diabetic skin wound healing model.[10] These reports together with the present Murakami's work point out the involvement of macrophage recruitment in lymphangiogenesis in certain conditions.

The scenario of angiogenesis and associating (or following) lymphangiogenesis may be as follows. The trigger of these phenomena should be the induction of VEGF-A. VEGF-A stimulates vascular ECs via VEGFR2 and that initiates angiogenesis. Simultaneously, VEGF-A induces the mobilization of bone marrow cells including monocytes via VEGFR1. Monocytes recruit to the area of angiogenesis, differentiate to macrophages, and produce both angiogenesis and lymphangiogenesis stimulators. Angiogenesis stimulators include VEGF-A, whereas lymphangiogenesis stimulators include VEGF-C and VEGF-D. Accordingly, VEGF-A from macrophages potentiates angiogenesis via VEGFR2 on vascular ECs, whereas VEGF-C and VEGF-D from macrophages induce lymphangiogenesis via VEGFR3 on lymphatic ECs. Of course, this scenario is drawn from data obtained by the models of pathological conditions. It is still unclear how physiological lymphangiogenesis is regulated. What cell type is the main source of VEGF-C and VEGF-D in the physiological condition? How is the expression of VEGF-C and VEGF-D regulated? Further studies are expected to resolve these questions.

Disclosures

None.

References

1. Alitalo K, Tammela T, Petrova TV. Lymphangiogenesis in development and human disease. *Nature*. 2005;438:946–953.
2. Ferrara N. Vascular endothelial growth factor: basic science and clinical progress. *Endocr Rev*. 2004;25:581–611.
3. Chilov D, Kukk E, Taira S, Jeltsch M, Kaukonen J, Palotie A, Joukov V, Alitalo K. Genomic organization of human and mouse genes for vascular endothelial growth factor C. *J Biol Chem*. 1997;272:25176–25183.
4. Tsai PW, Shiah SG, Lin MT, Wu CW, Kuo ML. Up-regulation of vascular endothelial growth factor C in breast cancer cells by heregulin-β1. A critical role of p38/nuclear factor-κB signaling pathway. *J Biol Chem*. 2003;278:5750–5759.
5. Timoshenko AV, Chakraborty C, Wagner GF, Lala PK. COX-2-mediated stimulation of the lymphangiogenic factor VEGF-C in human breast cancer. *Br J Cancer*. 2006;94:1154–1163.
6. Dirkx AE, Oude Egbrink MG, Wagstaff J, Griffioen AW. Monocyte/macrophage infiltration in tumors: modulators of angiogenesis. *J Leukoc Biol*. 2006;80:1183–1196.
7. Schoppmann SF, Birner P, Stöckl J, Kalt R, Ullrich R, Caucig C, Kriehuber E, Nagy K, Alitalo K, Kerjaschki D. Tumor-associated macrophages express lymphatic endothelial growth factors and are related to peritumoral lymphangiogenesis. *Am J Pathol*. 2002;161:947–956.
8. Schoppmann SF, Fenzl A, Nagy K, Unger S, Bayer G, Geleff S, Gnant M, Horvat R, Jakesz R, Birner P. VEGF-C expressing tumor-associated macrophages in lymph node positive breast cancer: impact on lymphangiogenesis and survival. *Surgery*. 2006;139:839–846.
9. Cursiefen C, Chen L, Borges LP, Jackson D, Cao J, Radziejewski C, D'Amore PA, Dana MR, Wiegand SJ, Streilein JW. VEGF-A stimulates lymphangiogenesis and hemangiogenesis in inflammatory neovascularization via macrophage recruitment. *J Clin Invest*. 2004;113:1040–1050.
10. Maruyama K, Asai J, Ii M, Thorne T, Losordo DW, D'Amore PA. Decreased macrophage number and activation lead to reduced lymphatic vessel formation and contribute to impaired diabetic wound healing. *Am J Pathol*. 2007;170:1178–1191.

Expression of vasohibin as a novel endothelium-derived angiogenesis inhibitor in endometrial cancer

Kousuke Yoshinaga,[1] Kiyoshi Ito,[1,4] Takuya Moriya,[2] Satoru Nagase,[1] Tadao Takano,[1] Hitoshi Niikura,[1] Nobuo Yaegashi[1] and Yasufumi Sato[3]

[1]Department of Gynecology and [2]Department of Pathology, Tohoku University Graduate School of Medicine, [3]Department of Vascular Biology, Institute of Development, Aging, and Cancer, Tohoku University, Seiryo-cho 1-1 Aoba ward, Sendai City, Japan

(Received September 13, 2007/Revised January 8, 2008/Accepted January 14, 2008/Online publication March 5, 2008)

We have previously reported on vasohibin as a novel endothelium-derived vascular endothelial growth factor (VEGF)–inducible inhibitor of angiogenesis. The aim of our present study was to define the role of vasohibin in endometrioid endometrial adenocarcinoma. We collected 78 sections of endometrial carcinoma for assessment using immunohistochemistry. Twenty-seven were well differentiated (G1), 25 were moderately differentiated (G2), and 26 were poorly differentiated endometrioid adenocarcinomas (G3). We also included 12 sections of normal cyclic endometria, six of which were in the proliferative phase and six were in the secretory phase. We investigated the expression of vasohibin, and compared it to VEGF receptor-2 (VEGFR-2: KDR/flk-1), CD34, Ki-67, VEGF-A, and D2-40 (as a lymphatic vessel marker). We assessed the ratio of vasohibin- and VEGFR-2-positive vessels in the stroma of endometrial carcinoma. Immunohistochemical assessment was classified as negative or positive based on staining intensity. Vasohibin was selectively expressed on vascular endothelial cells in both cyclic endometria and endometrial carcinomas. Vasohibin was highly expressed in the normal functional endmetrium of the secretory phase, especially in the spiral artery, and was highly expressed in all grades of endometrioid adenocarcinomas. The stromal endothelial cells in G3 expressed vasohibin and VEGFR-2 more frequently than these in G1. In endometrioid adenocarcinomas, there was a significant correlation between the expression percentage of vasohibin and that of VEGFR-2 ($P < 0.0001$, $r^2 = 0.591$). This is the first study to elucidate the correlation between expression of vasohibin in the stromal endothelial cells and that of VEGFR-2 in human carcinomas. (*Cancer Sci* 2008; 99: 914–919)

Endometrial carcinoma is one of the most common gynecologic malignancies in women worldwide, and its incidence, especially that of endometrioid endometrial carcinoma, has recently increased.[1] The morbidity of endometrial cancer is rapidly increasing in Japan. In order to predict the behavior of aggressive tumors, various factors and/or phenomena associated with endometrial cancer have been studied extensively. It is well recognized that angiogenesis, the process of formation of new vessels, is requisite for tumor growth and enables hematogenous spread of tumor cells throughout the body. Several studies have documented the association between the microvessel density (MVD) and/or the extent of endothelial proliferation and tumor stage, as well as recurrence of endometrial cancer.[2–7] Angiogenesis is determined by the local balance between angiogenic stimulators and inhibitors. The expression of various angiogenesis stimulators, such as vascular endothelial growth factors (VEGFs), angiopoietins, and thymidine phosphorylase, has been described in endometrial cancer.[8–12] However, the significance of endogenous angiogenesis inhibitors in endometrial cancer is poorly documented.

We recently isolated a novel angiogenesis inhibitor, vasohibin, which is specifically expressed in endothelial cells (ECs). Its basal expression in quiescent ECs is low, but it is induced in response to angiogenic stimuli, such as VEGF-A and fibroblast growth factor (FGF)-2, and inhibits angiogenesis in an autocrine manner.[13,14] We therefore propose that vasohibin inhibits angiogenesis as a negative feedback regulator. Among the VEGF family members, VEGF-A is the most important factor for angiogenesis, and most of the VEGF-A-mediated signals for angiogenesis are transduced via VEGF receptor-2 (VEGFR-2).[15] We observed that the VEGF-A-mediated induction of vasohibin was preferentially mediated via the VEGFR-2 signaling pathway.[16]

In the present study, we aimed to elucidate the significance of vasohibin in human endometrium and its disorder(s). We also studied MVD and lymphatic vessel density (LVD). Physiological periodic angiogenesis is observed in functional endometria. We therefore enrolled functional endometria and endometrioid adenocarcinoma, as endometriotic-type endometrial adenocarcinoma, and compared the expression of vasohibin and VEGFR-2. Our analysis revealed a significantly positive correlation between vasohibin and VEGFR-2 in endometrial cancer. This is the first study to profile the expression of vasohibin, a negative feedback regulator of angiogenesis, in gynecologic malignancy.

Materials and Methods

Tissue specimens and clinical data. Seventy-eight endometrioid endometrial carcinomas (27 well differentiated, 25 moderately differentiated, 26 poorly differentiated; 50 stage I, 3 stage II, 20 stage III, 5 stage IV) were retrieved from the surgical pathology files of Tohoku University Hospital, Sendai, Japan. The average age of the patients was 55.6 ± 10.7 years. The protocol for this study was approved by the Ethics Committee at Tohoku University School of Medicine (Sendai, Japan). Each patient provided written informed consent before her surgery. None of the patients examined had received irradiation, hormonal therapy, or chemotherapy prior to surgery. The clinicopathological findings of the patients, including age, histology, stage, grade, and preoperative therapy was retrieved by extensive review of the charts. A standard primary treatment for endometrial carcinoma at Tohoku University Hospital was surgery consisting of total abdominal hysterectomy, salpingo-oopholectomy, pelvic and/or para-aortic lymphadenectomy, and peritoneal washing cytology. The lesions were classified according to the Histological Typing of Female Genital Tract Tumors by the World Health Organization, and staged according to the International Federation of Gynecology and Obstetrics system.[17,18] Patients with subtypes other than endometrioid or

[4]To whom correspondence should be addressed.
E-mail: kito@mail.tains.tohoku.ac.jp

doi: 10.1111/j.1349-7006.2008.00777.x

with second primary carcinoma were excluded from this series, because the endometrioid type and the others are referred to as type 1 and type 2 endometrial cancer are considered to originate from different mechanisms and exhibit different clinical behaviors.[17]

We also examined 12 sections of normal cyclic endometria derived from surgically resected specimens for benign uterine diseases, six of which were in the proliferative phase and six of which were in the secretory phase. The average age of these patients was 38.7 ± 4.9 and 40.3 ± 6.1 years, respectively. All specimens were routinely processed (i.e. 10% formalin fixed for 24–48 h), paraffin embedded, and thin sectioned (3 μm).

Immunohistochemical staining and scoring of immunoreactivity. We performed immunohistochemical staining for vasohibin, VEGFR-2, CD34 as a marker for vascular endothelial cells, and D2-40 as a lymphatic vessel marker. Ki-67 and VEGF-A were investigated in endometrial carcinoma cells. Paraffin-embedded tissue sections from human endometrial cancers were deparaffinized, rehydrated, and incubated with 3% H_2O_2 for 10 min to block endogenous peroxidase activity. Sections were incubated for 30 min at room temperature (RT) in a blocking solution of 10% goat serum (Nichirei Biosciences, Tokyo, Japan), and then stained for 12 h at 4°C with primary antibodies, followed by staining for 30 min at RT with secondary antibodies. The primary antibodies were all mouse monoclonal antibodies and were used as follows: 2 μg/mL antihuman vasohibin monoclonal antibody, anti-VEGFR-2 (Santa Cruz Biotechnology, Santa Cruz, CA, USA) diluted 1:100, anti-CD34 (Dako, Copenhagen, Denmark) diluted at 1:200, Ki-67 (Dako) diluted 1:100, anti-D2-40 (Dako) diluted 1:100, and anti-VEGF-A (Lab Vision, Fremont, CA, USA) diluted 1:100. We have previously described a mouse monoclonal antibody against a synthetic peptide corresponding to the 286–299 amino acid sequence of vasohibin.[13] The positive control slide for CD34 antigen was prepared from paraffin-fixed breast cancer tissue that was known to contain a high microvessel density. Nuclei were counterstained with hematoxylin.

Three investigators (A.T., H.T., M.K.) independently evaluated the immunohistochemical staining of the tissue sections. They were blinded to the clinical course of the patients and the average of the numbers counted by the three investigators was adopted for subsequent analysis. We carefully selected for investigation areas where cancer cells came into contact with or invaded into the stroma. First, microvessels were counted by searching for CD34-positive signals after scanning the immunostained section at low magnification. The areas with the greatest number of distinctly highlighted microvessels were selected. Any cell clusters with CD34-positive signals were regarded as a single countable microvessel, regardless of whether a lumen was visible or not. Unstained lumina were considered artifacts even if they contained blood or tumor cells. Microvessel density (MVD) was assessed by light microscopy in areas of invasive tumor containing the highest numbers of capillaries and small venules per area (neovascular hot spots) according to the original method.[19] In endometrioid adenocarcinoma, the ratio of stroma per total area (as neovascular hot spots) decreased significantly with poorer histological differentiation. Thus, we measured the ratio of stroma per total area using National Institute of Health imaging (200 × magnification hot spot picture captured with Nikon imaging) and revised the true vessel counts per 1 mm^2 of stroma (microvessel density) for each case.

Investigation of lymphatic vessel density (LVD) was performed using the same procedure described as above, by searching for D2-40-positive signals.

Next, immunostaining for vasohibin and VEGFR-2 was evaluated in serial thin sections. Positive immunoreactive signals for vasohibin and VEGFR-2 in the CD34-positive microvessels were counted and calculated as positive ratios of vasohibin and VEGFR-2 in microvessels. Evaluation of Ki-67 immunoreactivity was performed at high-power field (400X) and used as a marker of cell proliferation. More than 500 tumor cells from each of three different representative fields were counted and the percentage of the number of positively stained nuclei relative to the total numbers of cells were determined as a labeling index (LI). The protein expression of selected angiogenic factor (VEGF-A) was examined by immunohistochemistry using an established antibody. For this marker, cytoplasmic staining intensity and the proportion of positive tumor cells were recorded and a staining index (values of 0–9) was calculated as the product of staining intensity (0–3) and the area of positive staining (1, <10%; 2, 10–50%; 3, > 50%).[20]

Statistical analysis. Statistical analysis, such as the Student's *t*-test and Peason's correlation coefficient test, were performed using StatView (version 4.5; SAS Institute Inc., Cary, NC, US). The results were considered significant when the *P*-values were <0.05.

Results

Microvessel density of endometrioid adenocarcinoma. CD34-positive microvessel density (counts per mm^2) were 41.1 ± 3.1, 36.9 ± 2.3, and 29.7 ± 1.7 in G1, G2, and G3, respectively; 35 ± 2.70 in the proliferative phase; and 36.3 ± 1.83 in the secretory phase (Figs 1 and 2). We measured the ratio of the stromal area per total hot spot area in the location with the greatest number of distinctly highlighted microvessels. In G1, the ratio was 32.7% ± 0.24; in G2, 27.5% ± 0.19; in G3, 5.8% ± 0.05; 73.2% ± 2.70 in the proliferative phase; and 70.0% ± 1.83 in the secretory phase. The ratio of the stromal area per total area of G3 was significantly lower than that of G1 and G2. CD34-positive microvessel density (counts per mm^2), as revised by the ratio of the stroma per total area, was 141.65 ± 13.2 in G1, 168.62 ± 19.38 in G2, and 788.94 ± 105.8 in G3, respectively; 48.71 ± 2.70 in the proliferative phase; and 52.45 ± 1.83 in the secretory phase. The MVD of G3 was significantly higher than the MVD of G1 and G2 (Fig. 3a).

Lymphatic vessel density of endometrioid adenocarcinoma. D2-40 positive lymphatic vessel density (counts per mm^2) was 4.73 ± 0.70 in G1, 8.83 ± 2.24 in G2, and 2.88 ± 0.54 in G3, respectively; 1.80 ± 0.20 in the proliferative phase; and 6.10 ± 0.50 in the secretory phase (Figs 1 and 2). D2-40 positive lymphatic vessel density (counts per mm^2), as revised by the ratio of stroma per total area, was 15.90 ± 2.30 in G1, 9.47 ± 1.95 in G2, and 91.01 ± 23.06 in G3, respectively; 2.53 ± 0.36 in the proliferative phase; and 8.83 ± 0.82 in the secretory phase. The LVD of G3 was significantly higher than the LVD of G1 and G2 (Fig. 3b).

Vasohibin expression in microvessels in endometrial tissues. The positive ratios of vasohibin in microvessels were 31.4% and 43.1% in the proliferative and secretory phases, respectively (Fig. 2). The positive ratios were significantly different between the two phases (Fig. 4a). In addition, the endothelium of the spiral arteries characteristically exhibited positivity in the secretory phase; the positive ratio of vasohibin was 95.4% and the positive ratio of VEGFR-2 was 87.4%. (Fig. 2).

The positive ratio of vasohibin in microvessels was 56.6% ± 12.8 in the endometrioid adenocarcinoma cases examined. Interestingly, the positive ratios differed according to grade: 52.5 ± 13.9 in G1 (well differentiated), 57.8% ± 13.5 in G2 (moderately differentiated), and 59.9% ± 10.0 in G3 (poorly differentiated) (Fig. 1). The positive ratio of vasohibin in microvessels in G3 was significantly higher than that in G1 (Fig. 4a). Positive ratios of vasohibin in microvessels in each histlogical grade were significantly higher than that of the proliferative phase ($P < 0.05$). Positive ratios were compared in clinical stages: 56.2% ± 11.2 in stage 1, 61.9% ± 15.5 in stage 2,

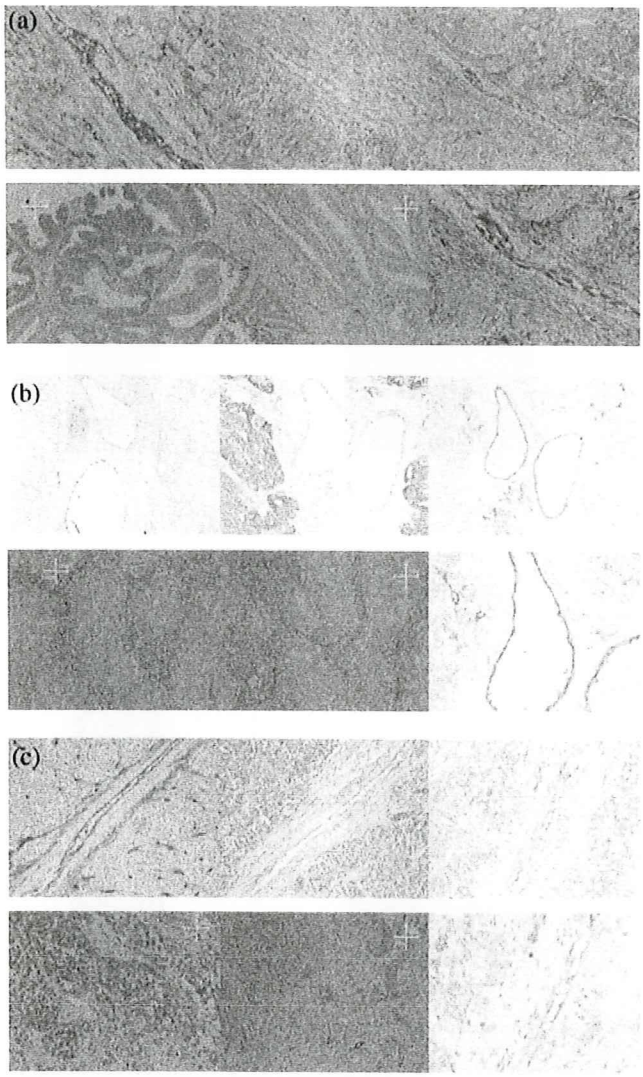

Fig. 1. (a) Immunohistochemistry in well-differentiated endometrioid adenocarcinomas. All sections stained positively for CD34 (upper left, original magnification 200×), vascular endothelial growth factor receptor-2 (VEGFR-2) (upper middle, original magnification 200×), vasohibin (upper right, original magnification 200× and lower right, original magnification 400×), and vascular endothelial growth factor-alpha (VEGF-A) (lower left, original magnification 200×). D2-40 (lower middle, original magnification 200×). (b) Immunohistochemistry in moderately differentiated adenocarcinoma. All sections stained positively as for (a). (c) Immunohistochemistry in poorly differentiated adenocarcinoma. All sections stained positively as for (a).

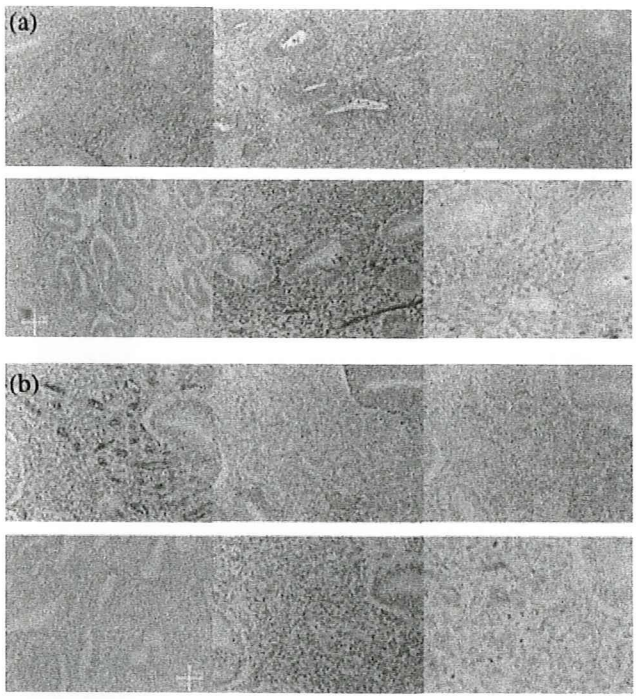

Fig. 2. (a) Immunohistochemistry in proliferative phase of cyclic endometria. All sections stained positively for CD34 (upper left, original magnification 200×), vascular endothelial growth factor receptor-2 (VEGFR-2) (upper middle, original magnification 200×), vasohibin (upper right, original magnification 200× and lower right, original magnification 400×), and vascular endothelial growth factor-alpha (VEGF-A) (lower left, original magnification 200×). D2-40 (lower middle, original magnification 200×). (b) Immunohistochemistry in secretory phase of cyclic endometria. All sections stained positively as for (a). Immunopositivity was significantly different between the two phases for vasohibin and VEGFR-2. The endothelium of the spiral arteries exhibited characteristic positivities in the secretory phase.

56.7% ± 12.9 in stage 3, and 57.7% ± 21.3 in stage 4. There was no significant difference between each group.

VEGFR-2 expression in microvessels in endometrial tissues. The VEGFR-2 positive ratio of the microvessels was 8.6% ± 1.0 and 22.5% ± 3.0 in the proliferative and secretory phases, respectively (Fig. 2). VEGFR-2 positive vessel ratio in the proliferative phase was significantly higher than in the secretory phase (Fig. 4b).

VEGFR-2 positive ratios in G1, 2, and G3 were 22.3% ± 13.0, 39.8% ± 12.8, and 47.6% ± 11.5, respectively (Fig. 1). The VEGFR-2 positive ratio in G2 was significantly higher than in G1 and cyclic endometria. The VEGFR-2 positive ratio in G3 was significantly higher than those of G1 and G2 (Fig. 4b). Positive ratios were compared between clinical stages: 32.8% ± 15.4% in stage 1, 33.9% ± 19.0 in stage 2, 37.5% ± 15.1 in stage 3, and 46.4% ± 16.8 in stage 4. There was no significant difference between each group.

VEGF-A expression in endometrial tissues. VEGF-A expression was detected in the cytoplasm of epithelial cells. The staining index of VEGF-A is shown in Figure 5. The VEGF-A positive ratio of cytoplasmic staining intensity was 0.67 ± 0.49 and 2.33 ± 0.76 in the proliferative and secretory phases, respectively (Fig. 5). In endometrioid adenocarcinomas VEGF-A positive ratios of cytoplasmic staining in grades 1, 2, and 3 were 3.85 ± 0.39, 4.2 ± 0.37, and 5.88 ± 0.37, respectively (Fig. 5). The VEGF-A positive ratio in G3 was significantly higher than in G1 and 2. The VEGF-A positive ratio in the proliferative phase was significantly lower than G1, G2, and G3, respectively, and the VEGF-A positive ratio in secretory phase was significantly lower than G2 and G3, respectively.

Correlation between vasohibin and VEGFR-2 positive ratios in microvessels, and cell proliferation and expression of angiogenic factor. A strongly positive correlation was found between vasohibin and VEGFR-2 positive ratios in microvessels in endometrioid adenocarcinomas ($P < 0.0001$, $r^2 = 0.591$) (Fig. 6).

We then analyzed vasohibin and VEGFR-2 positive ratios in comparison to cell proliferation and expression of angiogenic factor. The ratios of both vasohibin- and VEGFR-2-positivity did not correlate significantly to the LI of Ki-67 (data not

doi: 10.1111/j.1349-7006.2008.00777.x

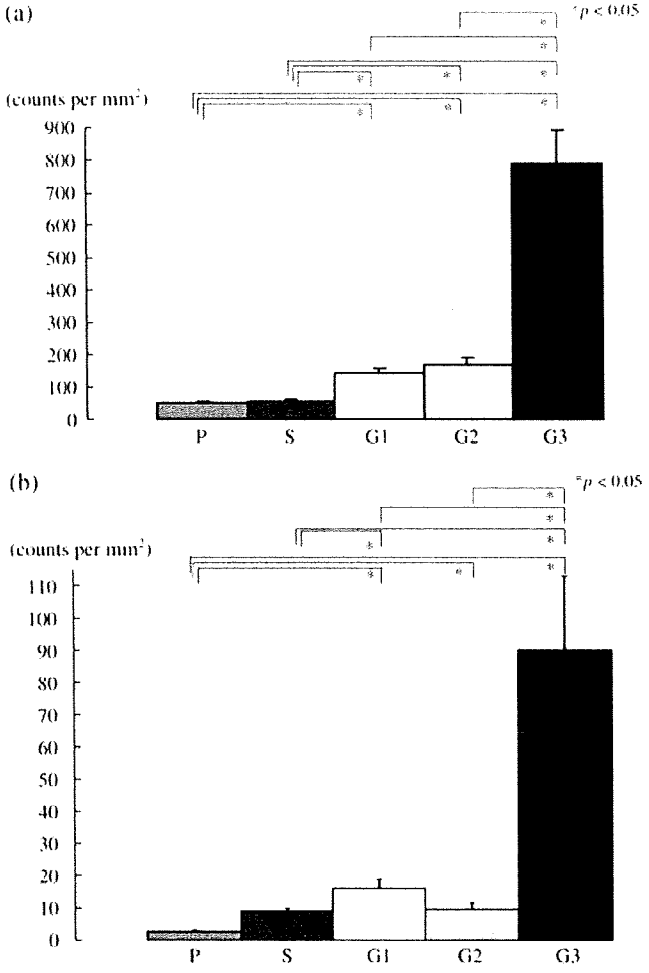

Fig. 3. (a) Microvessel density of cyclic endometria and endometrioid adenocarcinoma. Microvessel density of G3 was significantly higher than that of G1 and G2. G1, well-differentiated adenocarcinoma; G2, moderately differentiated adenocarcinoma; G3, poorly differentiated adenocarcinoma, $*P < 0.05$. (b) Lymphatic vessel density of cyclic endometria and endometrioid adenocarcinoma. Lymphatic vessel density of G3 was significantly higher than that of G1 and G2. G1, well-differentiated adenocarcinoma; G2, moderately differentiated adenocarcinoma; G3, poorly differentiated adenocarcinoma, $*P < 0.05$.

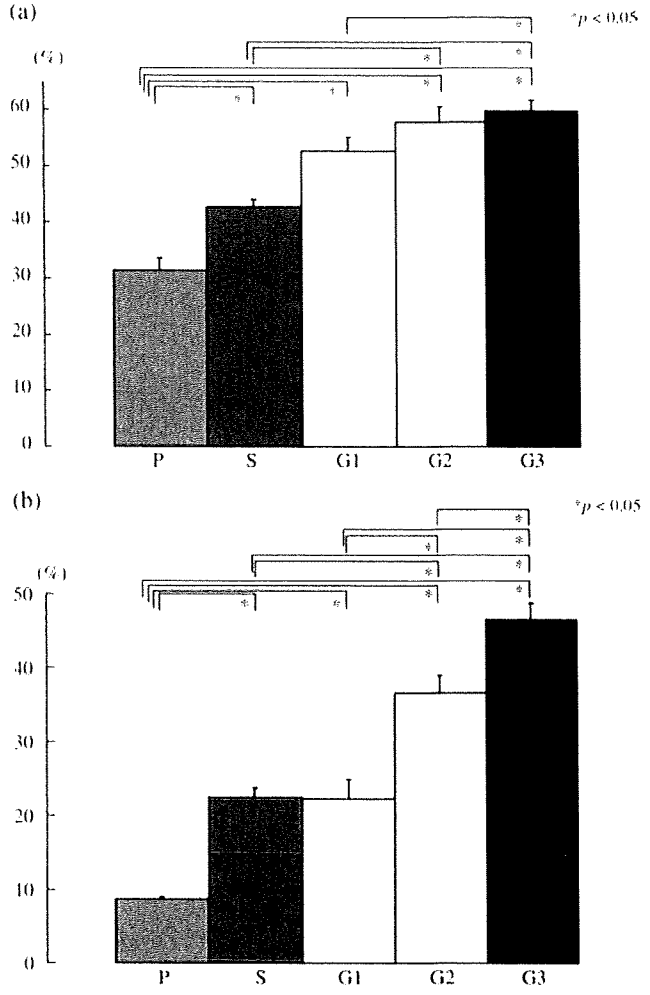

Fig. 4. (a) Proportion of vasohibin/CD34-positive vessels in cyclic endometria and endometrioid adenocarcinoma. Vasohibin-immunopositivity in microvessels in G3 was significantly higher than that in G1. S, secretory phase; P, proliferative phase; G1, well-differentiated adenocarcinoma; G2, moderately differentiated adenocarcinoma; G3, poorly differentiated adenocarcinoma, $*P < 0.05$. (b) Proportion of vascular endothelial growth factor receptor-2 (VEGFR-2)/CD34-positive vessels in cyclic endometria and endometrioid adenocarcinoma. VEGFR-2-immunopositivity of vessels in the proliferative phase was significantly higher than in the secretory phase. S, secretory phase; P, proliferative phase; G1, well-differentiated adenocarcinoma; G2, moderately differentiated adenocarcinoma; G3, poorly differentiated adenocarcinoma, $*P < 0.05$.

shown). No significant correlation was observed between the vasohibin- and VEGFR-2-positive ratios and VEGF-A expression in endometrioid adenocarcinoma (data not shown).

Discussion

Here we examined the vascular density of endometrial cancer and compared it with that of normal endometrium. Some reports have previously indicated that MVD of endometrial cancer increases from well differentiated to poorly differentiated adenocarcinomas[4,21,22] but this relationship is not universally accepted.[23] Moreover, most of them have failed to consider the vessel numbers in normal endometrium and to compare it with those of adenocarcinoma. In the present study, we confirmed that the vessel number increased from normal endometrium to endometrial cancer, and that this increase was significantly augmented in poorly differentiated adenocarcinoma.

Recently, focus has been given to the importance of lymphangiogenesis for tumor metastasis.[24,25] Here, we investigated LVD in normal endometrium and endometrioid adenocarcinoamas. Our analysis revealed that LVD increased significantly in poorly differentiated adenocarcinoma, similar to MVD. Some studies have reported the presence of peritumoral lymphatic vessels in 40% of the cases in endometrial cancer and demonstrated that high LVD was strongly associated with the features of aggressive endometrial carcinomas, including high histological grade, presence of necrosis, and vascular invasion by tumor cells.[26–28] Although it was expected that frequent LVD correlated with lymph node metastasis, there was no significant correlation between LVD and lymph node metastasis. In the present study, only two cases out of 78 cases exhibited lymph node metastasis. Therefore, investigation of a greater number of cases with lymph node metastasis in endometrioid adenocarcinoma will be necessary to further elucidate this correlation. The

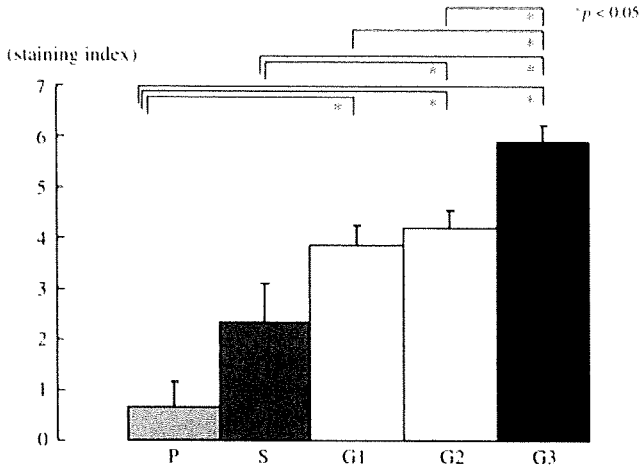

Fig. 5. Vascular endothelial growth factor-alpha (VEGF-A) staining indexes of the cytoplasm of the tumor cell and cyclic endometrial glands. $*P < 0.05$.

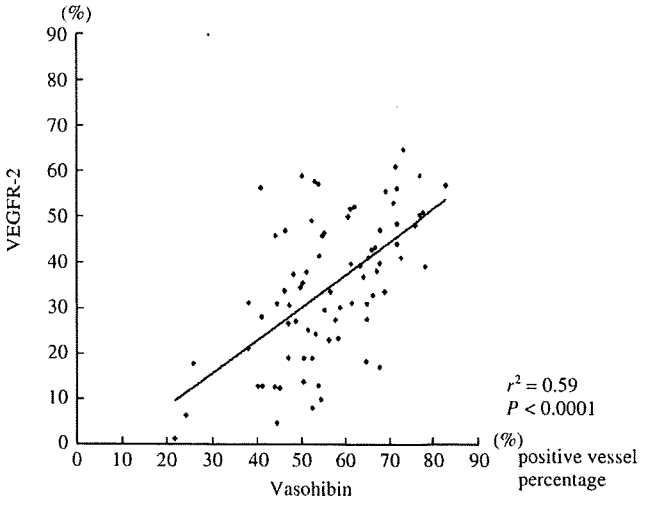

Fig. 6. Correlation between vasohibin and vascular endothelial growth factor receptor-2 (VEGFR-2). A strongly positive correlation was found between vasohibin- and VEGFR2-positive ratios in microvessels in endometrioid adenocarcinomas ($P < 0.0001$, $r^2 = 0.591$).

mechanism of the alteration of lymphangiogenesis from cyclic endometria to endometrioid adenocarcinoma remains unclear. Our analysis of MVD and LVD demonstrated that the secretory phase is similar to well differentiated and moderately differentiated endometrioid adenocarcinomas, which suggests that the function of cyclic endometria may be retained until adenocarcinomas become moderately differentiated.

We then examined the expression of vasohibin. Vasohibin is an endogenous endothelium-derived angiogenesis inhibitor that we have previously isolated.[13] Here we confirmed that the expression of vasohibin was restricted to vascular endothelium, and further observed that the ratio of vasohibin-positive vessels increased from normal endometrium to poorly differentiated adenocarcinomas. This is the first study to profile the expression of vasohibin in human gynecologic malignancy.

Several clinicopathologic studies have demonstrated a direct association between VEGF expression and increased MVD in human solid tumors, including breast[29] lung,[30] and gastric[31] malignancies. A similar association has been reported for normal[32] and malignant endometrium.[33–35] Between the two VEGF signal transducing receptors, VEGFR-2 transduces most of the angiogenesis-related signals in ECs. The VEGF/VEGFR-2 signaling pathway is also important for the induction of vasohibin in ECs.[16] We previously revealed that the VEGF-A-mediated induction of vasohibin was preferentially mediated via the VEGFR-2 signaling pathway.[16]

Our present analysis revealed that the ratio of VEGFR-2-positive vessels, as well as the ratio of vasohibin-positive vessels, also increased from normal endometrium to poorly differentiated endometrial adenocarcinomas. In addition, a significantly positive correlation existed between the positive ratios of vasohibin and VEGFR-2 expression in endometrioid endometrial carcinomas. This is the first study to elucidate this correlation between expression of these factors in human cancer. This result suggested the value of vasohibin as a biomarker of angiogenesis at least in endometrial cancer.

Angiogenesis is determined by the local balance between angiogenic stimulators and inhibitors. Therefore, one may anticipate the application of angiogenesis inhibitors towards antiangiogenic therapy for the treatment of human malignancies including endometrial cancer. A number of angiogenesis inhibitors have been investigated and identified, including pigment epithelium-derived factor (PEDF), angiostatin, endostatin, and thrombospondin-1 (TSP-1). Vasohibin is a newly identified negative feedback regulator for angiogenesis. We previously reported that transfection of Lewis lung carcinoma (LCC) cells with the vasohibin gene did not affect the proliferation of cancer cell *in vitro*, but did inhibit tumor growth and tumor angiogenesis *in vivo*.[13] The growth of vasohibin-producing LLC cells in mice was significantly attenuated. In addition, tumors of mock-transfectants contained large luminal vessels, whereas those of vasohibin-producing LLC cells contained very small vessels, even when the size of tumors did not differ extremely.[14] These results suggest that vasohibin may play a very important role in regulating tumor angiogenesis.

Among the various angiogenesis inhibitors, thrombospondin-1 (TSP-1) has been extensively studied in cancers, although the role of TSP-1 in endometrial tumor angiogenesis and progression still remains controversial.[36] The expression of TSP-1 in epithelial cells and/or caner cells is up-regulated by the tumor suppressor gene *p53*, and down-regulated by oncogenes such as Myc and Ras. Thus, the mutation of *p53* or activation of *myc* and *ras* results in the down-regulation of TSP-1, which may alter tumor growth by modulating angiogenesis in a variety of tumor types. Herein, we demonstrated that the expression of vasohibin increased in ECs of endometrial cancer. As the expression of vasohibin was restricted to normal ECs, the alteration of tumor suppressor gene and/or oncogenes in tumor cells would not influence the expression of vasohibin. However, angiogenesis inhibitors may function in a concerted manner. Therefore, vasohibin alone may not be sufficient to control tumor angiogenesis, if other inhibitors become deregulated.

Nevertheless, since the expression of vasohibin increased in correlation with that of VEGFR-2, vasohibin could be an important biomarker of angiogenesis in both normal endometrium and endometrial cancer. However, further investigations are required to clarify the precise roles of vasohibin in regulating antiangiogenic activity in normal endometrium and its disorders.

Acknowledgments

This study was supported by a grant-in-aid from the Kurokawa Cancer Research Foundation; a grant-in-aid for Scientific Research on Priority Areas from the Ministry of Education, Science, and Culture of Japan; a grant-in-aid from the Ministry of Health, Labor, and Welfare of Japan; and a 21st Century COE Program Special Research Grant (Tohoku University) from the Ministry of Education, Science, Sports, and Culture of Japan.

doi: 10.1111/j.1349-7006.2008.00777.x

References

1 Jemal A, Tiwari RC, Murray T *et al.* Cancer statistics, 2004. *CA Cancer J Clin* 2004; **54**: 8–29.
2 Abulafia O, Triest WE, Sherer DM, Hansen CC, Ghezzi F. Angiogenesis in endometrial hyperplasia and stage I endometrial carcinoma. *Obstet Gynecol* 1995; **86** (4): 479–85.
3 Kirschner CV, Alanis-Amezcua JM, Martin VG *et al.* Angiogenesis factor in endometrial carcinoma. a new prognostic indicator? *Am J Obstet Gynecol* 1996; **174**: 1879–82; discussion 1882–4.
4 Kaku T, Kamura T, Kinukawa N *et al.* Angiogenesis in endometrial carcinoma. *Cancer* 1997; **80**: 741–7.
5 Salvesen HB, Iversen OE, Akslen LA. Independent prognostic importance of microvessel density in endometrial carcinoma. *Br J Cancer* 1998; **77**: 1140–4.
6 de Gois Speck NM, Focchi J, Alves AC, Ribalta JC, Osorio CA. Relationship between angiogenesis and grade of histologic differentiation in endometrial adenocarcinoma. *Eur J Gynaecol Oncol* 2005; **26**: 599–601.
7 Stefansson IM, Salvesen HB, Akslen LA. Vascular proliferation is important for clinical progress of endometrial cancer. *Cancer Res* 2006; **66**: 3303–9.
8 Hirai M, Nakagawara A, Oosaki T, Hayashi Y, Hirono M, Yoshihara T. Expression of vascular endothelial growth factors (VEGF-A/VEGF-1 and VEGF-C/VEGF-2) in postmenopausal uterine endometrial carcinoma. *Gynecol Oncol* 2001; **80**: 181–8.
9 Fujisawa T, Watanabe J, Akaboshi M, Ohno E, Kuramoto H. Immunohistochemical study on VEGF expression in endometrial carcinoma – comparison with p53 expression, angiogenesis, and tumor histologic grade. *J Cancer Res Clin Oncol* 2001; **127**: 668–74.
10 Holland CM, Day K, Evans A, Smith SK. Expression of the VEGF and angiopoietin genes in endometrial atypical hyperplasia and endometrial cancer. *Br J Cancer* 2003; **89**: 891–8.
11 Saito M, Watanabe J, Fujisawa T *et al.* Angiopoietin-1, 2 and Tie2 expression in endometrial adenocarcinoma – the Ang2 dominant balance up–regulates tumor angiogenesis in the presence of VEGF. *Eur J Gynaecol Oncol* 2006; **27**: 129–34.
12 Mazurek A, Kuc P, Terlikowski S, Laudanski T. Evaluation of tumor angiogenesis and thymidine phosphorylase tissue expression in patients with endometrial cancer. *Neoplasma* 2006; **53**: 242–6.
13 Watanabe K, Hasegawa Y, Yamashita H *et al.* Vasohibin as an endothelium-derived negative feedback regulator of angiogenesis,. *J Clin Invest* 2004; **114**: 898–907.
14 Sonoda H, Ohta H, Watanabe K, Yamashita H, Sato Y. Multiple processing forms and their biological activities of a novel angiogenesis inhibitor Vasohibin. *Biochem Biophys Res Comms* 2006; **342**: 640–6.
15 Shibuya M, Claesson-Welsh L. Signal transduction by VEGF receptors in regulation of angiogenesis and lymphangiogenesis. *Exp Cell Res* 2006; **312**: 549–60.
16 Shimizu K, Watanabe K, Yamashita H *et al.* Gene regulation of a novel angiogenesis inhibitor, Vasohibin, in endothelial cells. *Biochem Biophys Res Commun* 2005; **327**: 700–6.
17 World Health Organization classification of tumours. In: Tavassoli FA, Devilee P, eds. *Pathology and Genetics of Tumours of the Breast and Female Genital Organs*. Lyon: IARC Press, 2003; 217–32.
18 Creasman WT. Announcement FIGO stages: 1988 revisions. *Gynecol Oncol* 1989; **35**: 125–7.
19 Weidner N, Semple JP, Welch WR, Folkman J. Tumor angiogenesis and metastasis – correlation in invasive breast carcinoma. *N Engl J Med* 1991; **324**: 1–8.
20 Aas T, Borresen AL, Geisler S *et al.* Specific P53 mutations are associated with de novo resistance to doxorubicin in breast cancer patients. *Nat Med* 1996; **2**: 811–4.
21 Wagatsuma S, Konno R, Sato S, Yajima A. Tumor angiogenesis, hepatocyte growth factor, and c-Met expression in endometrial carcinoma. *Cancer* 1998; **82**: 520–30.
22 Salvesen HB, Iversen OE, Akslen LA. Prognostic significance of angiogenesis and Ki-67, 53, and p21 expression: a population-based endometrial carcinoma study. *J Clin Oncol* 1999; **17**: 1382–90.
23 Morgan KG, Wilkinson N, Buckley CH. Angiogenesis in normal, hyperplastic, and neoplastic endometrium. *J Pathol* 1996; **179**: 317–20.
24 Alitalo K, Mohla S, Ruoslahti E. Lymphangiogenesis and cancer: meeting report. *Cancer Res* 2004; **64**: 9225–9.
25 Sipos B, Klapper W, Kruse ML *et al.* Expression of lymphangiogenic factors and evidence of intratumoral lymphangiogenesis in pancreatic endocrine tumors. *Am J Pathol* 2004; **165**: 1187–97.
26 Ingunn M, Stefansson Helga Salvesen B &, Lars Akslenl A. Vascular proliferation is important for clinical progress of endometrial cancer. *Cancer Res* 2006; **66**: 3303–7.
27 Bono P, Wasenius VM, Heikkila P *et al.* High LYVE-1-positive lymphatic vessel numbers are associatedwith poor outcome in breast cancer. *Clin Cancer Res* 2004; **10**: 7144–9.
28 Shields JD, Borsetti M, Rigby H *et al.* Lymphatic density and metastatic spread in human malignant melanoma. *Br J Cancer* 2004; **90**: 693–700.
29 Toi M, Inada K, Suzuki H, Tominaga T. Tumor angiogenesis in breast cancer: its importance as a prognostic indicator and the association with vascular endothelial growth factor expression. *Breast Cancer Res Treat* 1995; **36**: 193–204.
30 Giatromanolaki A, Koukourakis MI, Kakolyris S *et al.* Vascular endothelial growth factor, wild-type p53, and angiogenesis in early operable nonsmall cell lung cancer. *Clin Cancer Res* 1998; **4**: 3017–24.
31 Giatromanolaki A, Koukourakis MI, Stathopoulos GP *et al.* Angiogenic interactions of vascular endothelial growth factor, of thymidine phosphorylase, and of p53 protein expression in locally advanced gastric cancer. *Oncol Res* 2000; **12**: 33–41.
32 Charnock-Jones DS, Sharkey AM, Rajput-Williams J *et al.* Identification and localization of alternately spliced mRNAs for vascular endothelial growth factor in human uterus and estrogen regulation in endometrial carcinoma cell lines. *Biol Reprod* 1993; **48**: 1120–8.
33 Guidi AJ, Abu-Jawdeh G, Tognazzi K, Dvorak HF, Brown LF. Expression of vascular permeability factor (vascular endothelial growth factor) and its receptors in endometrial carcinoma. *Cancer* 1996; **78**: 454–60.
34 Fine BA, Valente PT, Feinstein GI, Dey T. VEGF, flt-1, and KDR/flk-1 as prognostic indicators in endometrial carcinoma. *Gynecol Oncol* 2000; **76**: 33–9.
35 Fujimoto J, Ichigo S, Hirose R, Sakaguchi H, Tamaya T. Expressions of vascular endothelial growth factor (VEGF) and its mRNA in uterine endometrial cancers. *Cancer Lett* 1998; **134**: 15–22.
36 Ren B, Yee KO, Lawler J, Khosravi-Far R. Regulation of tumor angiogenesis by thrombospondin-1. *Biochim Biophys Acta* 2006; **1765**: 178–88.

Expression of Vasohibin, an Antiangiogenic Factor, in Human Choroidal Neovascular Membranes

RYOSUKE WAKUSAWA, TOSHIAKI ABE, HAJIME SATO, MADOKA YOSHIDA, HIROSHI KUNIKATA, YASUFUMI SATO, AND KOHJI NISHIDA

• PURPOSE: To determine whether vasohibin, an antiangiogenic factor produced by vascular endothelial cells, is expressed in the choroidal neovascular (CNV) membranes obtained from human eyes with age-related macular degeneration (AMD) or polypoidal choroidal vasculopathy (PCV).

• DESIGN: Retrospective, interventional case series.

• METHODS: The medical charts of 21 eyes of 21 patients with AMD or PCV who underwent surgical removal of the CNV membrane were reviewed. The removed tissues were immunostained for von Willebrand Factor (vWF), vascular endothelial growth factor (VEGF), and vasohibin. The levels of the messenger ribonucleic acid of VEGF, VEGFR2, and vasohibin were determined by real-time reverse-transcriptase polymerase chain reaction (RT-PCR) from the CNV membranes excised from nine AMD and nine PCV patients.

• RESULTS: The patients were divided into three groups; four patients were placed in the most active group (Group H), 13 in the less active group (Group E), and four in the nonactive group (Group S). Immunohistochemistry showed that vasohibin, vWF, and VEGF were expressed in the vascular endothelial cells in the CNV membranes and in the polypoidal vessels. RT-PCR showed that there was a strong correlation between the level of expression of VEGFR2 and vasohibin ($P = .0002$). Eyes with a lower vasohibin-to-VEGF ratio tended to have larger subretinal hemorrhages or vitreous hemorrhages, whereas eyes with higher vasohibin-to-VEGF ratio had subretinal fibrosislike lesions. Statistical analysis of the vasohibin-to-VEGF ratio among the three groups was significant ($P = .0209$).

• CONCLUSIONS: Vasohibin is expressed in human CNV membranes. Our results indicate that the vasohibin-to-VEGF ratio may be related with the activity of the CNV.

AJO.com Supplemental Material available at AJO.com.
Accepted for publication Mar 13, 2008.

From the Department of Ophthalmology and Visual Science (R.W., H.S., Y.M., H.K., K.N.); the Division of Clinical Cell Therapy, Center for Translational and Advanced Animal Research (T.A.); and the Department of Vascular Biology, Institute of Development, Aging, and Cancer (Y.S.), Tohoku University Graduate School of Medicine, Miyagi, Japan.

Inquires to Ryosuke Wakusawa, Department of Ophthalmology and Visual Science, Tohoku University Graduate School of Medicine, 1-1, Seiryo-cho, Aoba-ku, Sendai 980–8574, Miyagi, Japan; e-mail: ckd19390@rio.odn.ne.jp

(Am J Ophthalmol 2008;146:235–243. © 2008 by Elsevier Inc. All rights reserved.)

THREE FACTORS HAVE BEEN SUGGESTED TO CONTROL vasculogenesis and angiogenesis. These factors are: vascular endothelial growth factors (VEGFs) and VEGF receptors, angiopoietins (Ang) and Tie receptors, and the ephrins and Eph receptors.[1,2] The Ang–Tie system stabilizes the vascular wall, and the ephrin-B2–EphD4 system is required for the differentiation of vascular endothelial cells (ECs) during the earliest stages of arterial and venous development. The VEGFs and VEGF receptors play important roles in vasculogenesis, angiogenesis, and stabilization of mature vessels. VEGF receptor 2 (VEGFR2) is well accepted as the receptor that mediates functional VEGF signaling in ECs.

Neovascularization is the major cause of blindness in many ocular diseases. Age-related macular degeneration (AMD) is the most common cause of central vision loss in the elderly population of developed countries,[3] and the development of choroidal neovascularizations (CNVs) is characteristic of the exudative form of AMD. A CNV leads to subretinal hemorrhages, exudative lesions, serous retinal detachment (RD), and disciform scars.[4]

Endothelial cells, retinal pigment epithelial (RPE) cells, and macrophage-like mononuclear cells have been reported to be the major cellular components of CNV membranes, and they produce many different kinds of proangiogenic and antiangiogenic factors.[5–12] VEGF is one of the proangiogenic factors that plays major roles in the development of CNVs.[13]

Polypoidal choroidal vasculopathy (PCV), first described by Yannuzzi and associates, is characterized by an abnormal network of choroidal vessels with polyp-like dilations at the terminals of the branches.[14] Whether PCV represents a kind of CNV is still being debated, but PCV resembles AMD clinically and is relatively more common in the Japanese[15] and Chinese persons than in White persons.[16] Recent studies have demonstrated that VEGF was expressed in the ECs and RPE cells of a PCV lesion.[11]

Vasohibin recently was reported to be a VEGF-inducible gene in human cultured ECs,[17] and it is a secretory protein made up of several processed forms, for example, 27, 32, 36, 42, and 44 kDa.[18] It has been reported that recombinant vasohibin inhibited the network formation of ECs in

0002-9394/08/$34.00
doi:10.1016/j.ajo.2008.03.019

TABLE 1. Clinical Characteristics of 11 Patients with Age-Related Macular Degeneration and 10 with Polypoidal Choroidal Vasculopathy

Case No.	Age (yrs)	Gender	Diagnosis	TAP Classification	Lesion Size*	Subgroup	Analysis
1	56	M	AMD	Predominantly classic	0.9	E	IHC
2	72	M	AMD	Minimally classic	2.8	E	IHC
3	73	F	PCV	Occult	3.4	E	IHC
4	76	M	AMD	Minimally classic	4.0	H	RT-PCR
5	65	M	AMD	Occult	4.8	H	RT-PCR
6	49	F	AMD	Predominantly classic	1.3	E	RT-PCR
7	85	M	AMD	Predominantly classic	3.1	E	RT-PCR
8	68	F	AMD	Minimally classic	2.7	E	RT-PCR
9	64	M	AMD	Minimally classic	3.3	E	RT-PCR
10	78	M	AMD	Minimally classic	4.1	E	RT-PCR
11	73	M	AMD	Staining†	1.4	S	RT-PCR
12	65	M	AMD	Staining†	1.9	S	RT-PCR
13	76	M	PCV	Occult	6.2	H	RT-PCR
14	56	M	PCV	Vitreous hemorrhage‡		H	RT-PCR
15	69	M	PCV	Minimally classic	2.1	E	RT-PCR
16	77	M	PCV	Minimally classic	3.0	E	RT-PCR
17	73	F	PCV	Occult	1.1	E	RT-PCR
18	65	M	PCV	Occult	2.0	E	RT-PCR
19	66	F	PCV	Occult	2.2	E	RT-PCR
20	66	M	PCV	Staining†	1.8	S	RT-PCR
21	72	M	PCV	Staining†	3.2	S	RT-PCR

AMD = age-related macular degeneration; F = female patients; Group E = exudative lesion excluded in subgroup H; Group H = massive subretinal hemorrhage or vitreous hemorrhage; Group S = quiescent lesion including disciform scar; IHC = immunohistochemistry; M = male; PCV = polypoidal choroidal vasculopathy; TAP = Treatment of Age-Related Macular Degeneration with Photodynamic Therapy Study; RT-PCR = reverse-transcriptase polymerase chain reaction.

*In disk diameters.

†Not applicable to TAP classification because of quiescent lesion.

‡Not applicable to TAP classification because of dense vitreous hemorrhage. Diagnosed with angiography before vitreous hemorrhage.

vitro[17] and also inhibited the retinal neovascularizaion in the mouse model of oxygen-induced ischemic retinopathy.[19] Vasohibin is different from other angiogenic inhibitors because it is induced selectively in ECs by proangiogenic factors such as VEGF and basic fibroblast growth factor (bFGF).[17,20] Vasohibin is considered to be an intrinsic and highly specific negative feedback regulator of activated ECs engaged in the process of angiogenesis.

The purpose of this study is to determine whether vasohibin is expressed in human CNV membranes obtained from eyes with AMD or PCV. We also examined the relationship between the degree of expression of vasohibin, VEGF, and VEGFR2 and considered whether the level of expression of these genes was related to the clinical manifestations among the patients.

METHODS

• SUBJECTS AND TREATMENTS: We reviewed the medical records of 11 eyes of 11 AMD patients and 10 eyes of 10 PCV patients who had undergone vitrectomy and surgical removal of a CNV with or without autologous iris pigment epithelial cell transplantation.[21] These were the initial treatment and were performed between May 10, 1996 and April 15, 2003. Photodynamic therapy was not available in Japan at that time.

In addition to the routine ophthalmologic examination, fluorescein angiography and indocyanine green angiography (ICGA) were performed on all patients, and optical coherence tomography (OCT) was performed on 12 patients before and after the surgery. The criteria used to determine whether surgery was required were: best-corrected visual acuity (BCVA) less than 0.2, progressive deterioration of vision during the three months before surgery, and other factors as described.[21]

The eyes were classified retrospectively into three subgroups according to the clinical findings: eyes in Group H had massive subretinal hemorrhage that extended beyond the temporal retinal vessel arcade or a vitreous hemorrhage; eyes in Group E had active exudative lesions such as subretinal hemorrhage, hard exudates, and serous RD within the vascular arcade; and eyes in Group S had resolved and no exudative lesions at the time of surgery,

but these patients had undergone surgery for the transplantation of autologous iris pigment epithelial cells. The clinical characteristics of the patients are summarized in Table 1.

• TISSUE PREPARATION AND IMMUNOHISTOCHEMISTRY: The CNV membranes from two patients with AMD and one patient with PCV were fixed in 4% formalin and embedded in paraffin. Serial 5-μm sections were cut, and adjacent sections were stained with hematoxylin and eosin.

Immunohistochemical staining for the von Willebrand Factor (vWF), VEGF, and vasohibin was performed using the horseradish peroxidase (HRP) method. All steps were performed at room temperature unless otherwise stated. Briefly, sections were deparaffinized, rehydrated, and then treated with 3% hydrogen peroxide to block endogenous peroxidase activity. After blocking with 1% bovine serum albumin in phosphate buffered saline (PBS) for 30 minutes, rabbit polyclonal antibodies against vWF (1:500; DAKO, Glostrup, Denmark), rabbit polyclonal antibodies against VEGF (1:200; Santa Cruz Biotechnology, Santa Cruz, California, USA), or mouse monoclonal antibodies against vasohibin (1:1000; made by Watanabe and associates) were applied to the sections overnight at 4 C.[17] The following morning, the sections were incubated in biotin-conjugated antirabbit immunoglobulin (Ig) G or anti-mouse IgG antibodies (Vector Laboratories, Burlingame, California, USA) for 30 minutes. The slides then were incubated with HRP-conjugated streptavidin (Vector Laboratories) for 30 minutes. Brown chromogen diaminobenzidine (Sigma-Aldrich, St Louis, Missouri, USA) was used for all sections. The sections were washed three times with PBS between each step. For control, preimmune rabbit IgG or mouse IgG was used instead of the primary antibody. Sections were examined under a standard light microscopy.

• PREPARATION OF TOTAL RIBONUCLEIC ACID AND REAL-TIME REVERSE-TRANSCRIPTASE POLYMERASE CHAIN REACTION: The CNV membranes from nine eyes with AMD and from nine eyes with PCV were separately mixed with denaturing solution, and messenger ribonucleic acid (mRNA) was prepared using QuickPrep micromRNA Purification Kit (Amersham Biosciences, Buckinghamshire, United Kingdom) according to the manufacturer's instructions. The purified mRNA was reverse-transcribed into complementary deoxyribonucleic acid (cDNA) using First-Strand cDNA Synthesis Kit (Amersham Biosciences). One microliter of cDNA was used for real-time reverse-transcriptase polymerase chain reaction (RT-PCR) amplification using a Light Cycler (Roche, Meylan, France) and the Light Cycler FastStart DNA Master SYBR Green I reagent Kit (Roche).

The primers for VEGF[22] and VEGFR2[12] were synthesized from the reported sequences. Primers for vasohibin and glyceraldehyde-3-phosphate-dehydrogenase (GAPDH) were designed to be intron spanning to preclude amplification of genomic DNA using GeneWorks version 2.45N (IntelliGenetics; Mountain View, California, USA) computer software.

TABLE 2. Semiquantitative Reverse-Transcriptase Polymerase Chain Reaction Conditions Used for the Amplification of Vasohibin and Other mRNAs

Gene	Sequence of Primers	Annealing Temperature
Vasohibin	5′-CTTACCTGCTTGCTGTCTGC-3′	59 C
	5′-CATGGATGGTGACTAAGGCC-3′	
VEGF	5′-GCAGAATCATCACGAAGTGG-3′	58 C
	5′-AAGGACTGTTCTGTCGATGG-3′	
VEGFR2	5′-CCAGATGAACTCCCATTGGATG-3′	56 C
	5′-CTCTTGCTCCTCAGGTAAGTGGAC-3′	
GAPDH	5′-AAGGTGAAGGTCGGAGTCAA-3′	55 C
	5′-TTGAGGTCAATGAAGGGGTC-3′	

GAPDH = glyceraldehyde-3-phosphate-dehydrogenase; mRNA = messenger ribonucleic acid; VEGF = vascular endothelial growth factor; VEGFR2 = vascular endothelial growth factor receptor 2.

The sequence of the primers and the experimental conditions for optimized amplification are summarized in Table 2. PCR conditions were: step 1, 95 C for 10 minutes; step 2, 95 C for 10 seconds; hybridization temperature as indicated in Table 2 for 10 seconds; and 72 C for 10 seconds. Step 2 was repeated for 45 cycles. All data were normalized to the GAPDH transcript level, thus giving the relative transcript level.

The relative transcript level of VEGF, VEGFR2, and vasohibin obtained from the CNV membranes of eyes with AMD or PCV were compared using the Mann–Whitney *U* test. The correlations between the transcription level of VEGF, VEGFR2, and vasohibin were calculated by the Pearson simple correlation coefficient. The relative transcript level of vasohibin and the transcription ratio of vasohibin to VEGF also were compared among Groups H, E, and S using Mann–Whitney *U* test.

RESULTS

• CLINICAL CLASSIFICATION AND CHARACTERIZATION: The 21 eyes (11 with AMD and 10 with PCV) were divided into three groups according to the clinical findings: Group H included four eyes that had the most active lesions, Group E had 13 eyes with less active lesions, and Group S had four eyes whose lesion were not active (Table 1). The median visual acuity was 0.02 in Group H, 0.04 in Group E, and 0.05 in Group S. The median size of the CNV estimated from the ICGA images[23] was 2.4 disk diameters (DD) in Group H, 1.3 DD in Group E, and 1.7

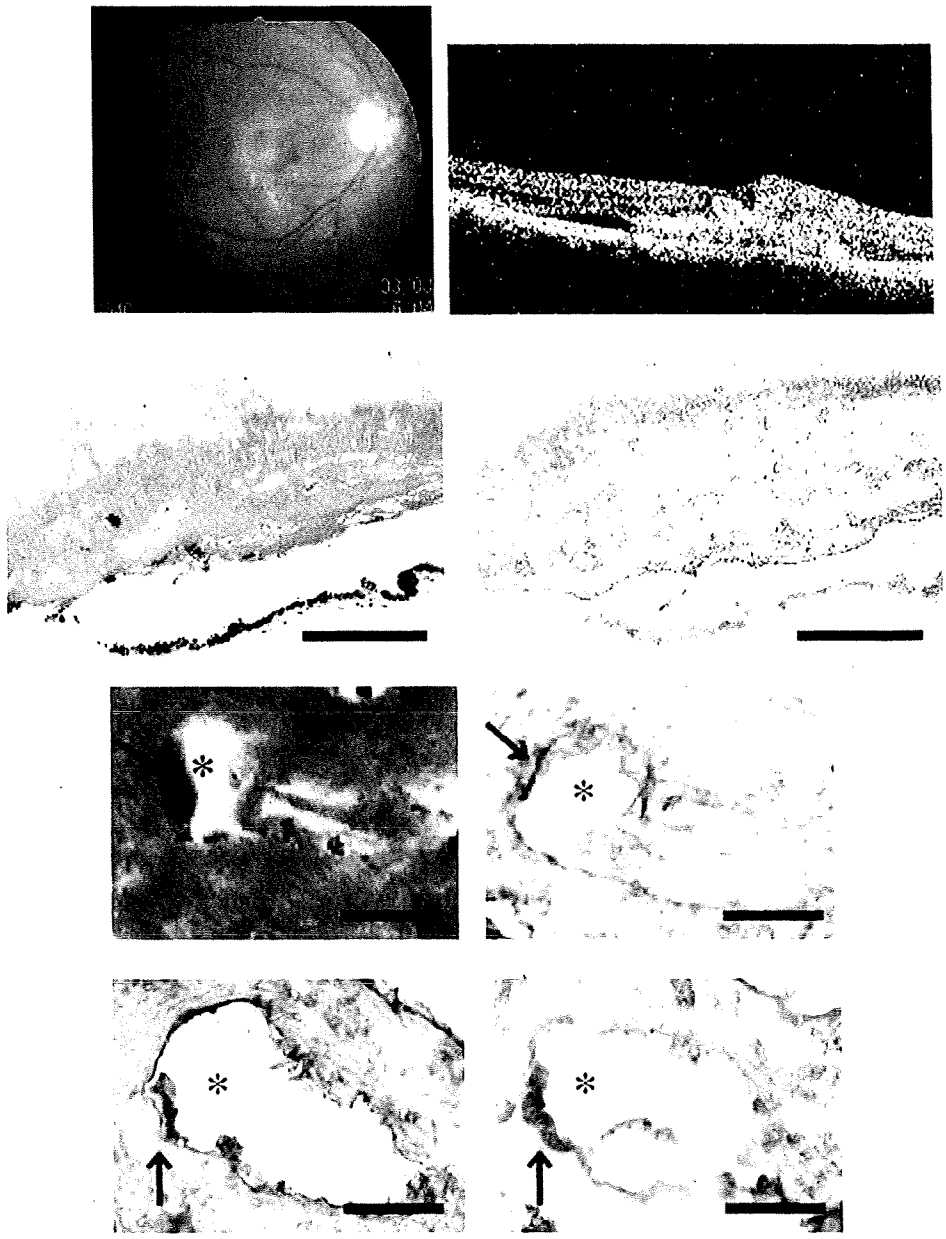

FIGURE 1. Images demonstrating the expression of vasohibin on the vascular endothelial cells (ECs) within the choroidal neovascularization (CNV) membrane obtained from an eye with age-related macular degeneration [AMD] (Cases 1 and 2 in Table 1). (Top left) Case 1: fundus photograph showing exudative lesion with subretinal hemorrhage. (Top right) Case 1: optical coherence tomogram showing CNV above the retinal pigment epithelium (RPE) layer. (Second row left) Photomicrograph of CNV membrane from Case 1 showing fibrovascular tissue beneath the outer segments of the photoreceptors. The brown linear structure under the CNV membrane is a sheet of RPE cells (stain, hematoxylin and eosin; original magnification, ×200). (Second row right) Photomicrograph showing vasohibin of CNV membrane from Case 1. Vasohibin is expressed on vascular ECs and some of the photoreceptor outer segments (stain, immunohistochemical staining for vasohibin; original magnification, ×200). (Third row left) Photomicrograph showing CNV membrane from Case 2 (stain, hematoxylin and eosin; original magnification, ×400). (Third row right) Photomicrograph showing vasohibin in CNV membrane from Case 2 (stain, immunohistochemical staining for vasohibin, original magnification, ×400). (Bottom left) Photomicrograph showing von Willebrand Factor (vWF) original magnification, ×400 in Case 2. (Bottom right) Photomicrograph showing vascular endothelial growth factor (VEGF) in Case 2 (stain, immunohistochemical staining for VEGF; original magnification, ×400). Arrows point to vascular ECs that are positive for each staining. Asterisks indicate the vessel lumens. Bar = 200 μm (second row); 20 μm (third row and bottom).